UNIVERSIDADE DA BEIRA INTERIOR
Engenharia

Exergy Analysis of a Turbofan Engine

(Versão final após defesa)

Diogo Neves Morais Paulo

Dissertação para obtenção do Grau de Mestre em
Engenharia Aeronáutica
(Ciclo de Estudos Integrado)

Orientador: Prof. Doutor Francisco Miguel Ribeiro Proença Brójo

Covilhã, Janeiro de 2018

Dedication

To my family and friends.

Acknowledgements

The author would like to thank Pr. Dr. Francisco Brójo, of the department of Aerospace Sciences of the University of Beira Interior, for his guidance and help in elaboration of this thesis.

The author would like to thank to his family and friends for their important support in the concretisation of this thesis.

Resumo

Nesta tese, é realizado um estudo exergético, aplicado a um motor turbofan de alta razão de bypass, para as condições de voo de cruzeiro. A análise exergética é considerada uma "ferramenta" extremamente importante, utilizada no design, operação e performance de sistemas energéticos. Entre todas as suas vantagens, é principalmente utilizada para determinar e calcular as localizações, tipos e magnitudes das perdas e destruições de exergia num sistema energético.

O motor escolhido para a análise exergética, foi o motor turbofan CFM56-5A1. Este motor é constituído por dois eixos, sendo que os componentes que foram submetidos à análise são respetivamente o fan, compressor de baixa pressão, compressor de alta pressão, câmara de combustão, turbina de alta pressão e turbina de baixa pressão.

De forma a realizar a análise exergética, foi necessário primeiro criar um modelo matemático do motor, com o fim de gerar os dados de performance do motor para as condições de cruzeiro. A modelação foi feita com recurso a um código criado no software Matlab R2015A. Adicionalmente foi utilizado o software Gasturb 13, como método de comparação e validação dos dados gerados do código em Matlab.

Na análise exergética, os componentes do motor foram definidos com recurso a equações de balanço de massa, energia e exergia. As figuras de mérito utilizadas para avaliar exergeticamente o motor, foram respectivamente a eficiência exergética, potencial de melhoramento, destruição de exergia relativa, "fuel depletion ratio" e "productivity lack".

Após realizada a análise exergética, o componente determinado como o mais irreversível foi a câmara de combustão, com uma destruição de exergia de 9.31 MW. As eficiências exergéticas do fan, LPC, HPC, CC, HPT, LPT, são respetivamente 92.13%, 95.91%, 97.52%, 76.71%, 90.74%, 90.32%.

Palavras-chave

Aviação, Exergia, Motor, Simulação, Turbofan

Abstract

In this thesis, exergetic methodology is applied to a high bypass turbofan engine at cruise flight phase. Exergy analysis is a powerful tool, which has been used in the design, operation, and performance of energy systems by many engineers and researchers. Among its advantages, it is primary used since it allows the determination of the locations, types, and true magnitudes of wastes and destruction of exergy.

The engine selected for this analysis, is the CFM56-5A1 turbofan engine. It has two spools and the components that are exergetically evaluated are the fan, low pressure compressor, high pressure compressor, combustion chamber, high pressure turbine and low pressure turbine.

In order to perform an exergy analysis, the modelling of the engine has to be performed first, for the cruise mission. It is modelled by using a genuine code in the software Matlab R2015A and was verified and validated by using the software Gasturb 13.

Next, the exergy analysis is performed according to the thermodynamic laws. The exergy analysis is carried out by conducting mass, energy and exergy balance of each component of the engine. The figures of merit used to evaluate the engine are as follows: exergy efficiency, improvement potential, relative exergy destruction, fuel depletion rate and productivity lack.

The most irreversible component of the engine is found to be the combustion chamber with 9.31 MW. The exergetic efficiencies of the fan, LPC, HPC, CC, HPT and LPT are 92.13%, 95.91%, 97.52%, 76.71%, 90.74%, 90.32%, respectively.

Keywords

Aviation, Engine, Exergy, Modelling, Turbofan

Contents

List of Figures

List of Tables

List of Acronyms

BDE	Burner Design Efficiency
BDER	Bypass Duct Expansion Ratio
CC	Combustion Chamber
ER	Expansion Ratio
HPC	High Pressure Compressor
HPCPR	High Pressure Compressor Pressure Ratio
HPT	High Pressure Turbine
HPTER	High Pressure Turbine Expansion Ratio
IAW	In Accordance With
ICAO	International Civil Aviation Organization
IFPR	Inner Fan Pressure Ratio
IPCC	Intergovernmental Panel on Climate Change
LPC	Low Pressure Compressor
LPT	Low Pressure Turbine
LPCPR	Low Pressure Compressor Pressure Ratio
LPTER	Low Pressure Turbine Expansion Ratio
NE	Nozzle Efficiency
OFPR	Outer Fan Pressure Ratio
PR	Pressure Ratio
TSFC	Thrust Specific Fuel Consumption

1 Introduction

1.1 Motivation

Air transportation plays a vital role in today`s society in the transportation of passengers and goods. With over two billion people traveling safely around the world every year and an average of 23000 aircraft in commercial service, worldwide passengers will average 5.1% growth and cargo traffic will average 5.6% growth [1].

On the other hand, the developments and growth in air transportation ultimately raises climate concerns. As the engine being the most pollutant component, aircraft engines produce gas pollutants, as CO_2, NO_x and other greenhouse gases, and contrails. The Forth Assessment Report (IPCC AR4) [2], a comprehensive assessment with the aim of studying the impact of aviation emissions, requested by ICAO and published in 2007, states that:

- Total CO_2 aviation emissions is approximately 2% of the global greenhouse gases emissions.
- The amount of CO_2 emissions from aviation are expected to grow around 3-4 percent per year.

However, air transportation is not compromised, as the environmental impact of emissions can be reduced by increasing the efficiency of resource utilization. Using energy more efficiently reduces pollutant emissions. Therefore, energy consumption plays a crucial importance role to achieve sustainable development, balancing economic and social development with environmental protection. More efficient energy systems must be developed, in order to achieve that.

Typically, engineering companies use energy analysis to assess and study energy systems. On the other hand, exergy analysis, as it is going to be discussed in this thesis, is better to evaluate the efficiency of energy systems.

Exergy analysis is a method that uses the conservation of mass and conservation of energy principles, together with the Second Law of Thermodynamics, for the analysis, design, and improvement of energy and other systems. The exergy method is a useful tool for furthering the goal of more efficient energy-resource use, since it can identify the locations, types, and magnitudes of wastes and losses and calculate meaningful efficiencies.

1.2 Objectives

The main objective of this thesis is to conduct an exergy analysis of an energy system, in this case, a turbofan engine, as it is by far the most commonly used engine in commercial aviation.

Using exergy approach, it will be possible to better understand the magnitudes of the exergy destruction and the inefficiencies of the various components within the engine.

It is important to refer that the engine will be evaluated exergetically for a specific operating condition, in this case, for the cruise flight conditions. Consequently, this raised a huge holdback. Due to product secrecy policies, the engine manufacturers don't provide any operating data of their engines, except for the engine specifications. Therefore, it was developed a mathematical model of the engine, to perform a simulation and generate the cruise operating data to be later used in the exergy analysis.

In brief, the objectives of this thesis are:

- To create a mathematical model of the energy system, in this case the turbofan engine, in order to perform a simulation and acquire the performance data for the cruise operating conditions.
- To conduct an exergy analysis of the turbofan engine.
- To determine the quantities and locations of exergy destruction, as well as using figures of merit to evaluate the turbofan engine.

1.3 Thesis Structure

The 1st chapter presents the motivation and objectives of the thesis.

The 2nd chapter describes the relevant studies related to the exergy analysis.

The 3rd chapter includes the modelling of the case study. It is presented the selected engine and it is described the theoretical bases and methodology to model the engine. The engine was first modelled using a genuine code and then was modelled using a professional software, and finally both results were compared in order to validate the genuine code results.

The 4th chapter describes the fundamentals of exergy. It is provided the theoretical background of exergy, the basic principles and formulas, general definitions, advantages, the implications, and others.

The 5th chapter presents the necessary equations applied to each component of the engine to perform the exergy analysis. It explains also the flows of exergy entering and exiting in each component.

The 6th chapter presents the results of the exergy analysis.

The 7th and final chapter presents the author's conclusions of the conducted study and also the future works related to exergy analysis.

2 Literature Review

2.1 Dr. Ibrahim Dincer Contribution to Exergy Researches

The author of this thesis considered relevant to mention Dr. Ibrahim Dincer. He dedicated his academic and scientific career studying exergy. He has made innovative contributions to the understanding and development of exergy analysis of advanced energy systems for his so-called five main pillars: better efficiency, cost-effectiveness, better environment, better sustainability, and better energy security. He is the author of hundreds of publications related to exergy, but the most important for this thesis were "Exergy: Energy, Environment And Sustainable Development" [3] and "Progress in Exergy, Energy, and the Environment" [4]. These books had an important impact in the development of this thesis since it explains the basic principles of exergy and the basis on how to conduct a well-structured exergy analysis.

2.2 Relevant Studies

In the recent years, some studies have been performed by researchers to evaluate the performance of energy systems based on the concept of exergy.

Ibrahim et al. [4] presented an exergy analysis of a low bypass turbofan engine at takeoff condition. The engine is the Pratt & Whitney JT8D, a low-bypass turbofan engine and its variants fitted to the 737-100/. At the end of the analysis, the most irreversible units in the system are found to be the combustor and the fan.

Tatiana et al. [5] performed an exergy analysis on an open gas turbine system. They demonstrated the importance of studying the thermodynamic performance of a system component, in order to determine which component of the system was causing exergy destruction.

Habib et al. [6] presented an exergy analysis of a cogeneration system. The analysis quantifies the irreversibilities of the different components of each plant. Additionally, the influence of the heat-to-power ratio and the process pressure on the thermal efficiency and utilization factor is presented. The results showed that the total irreversibility of the cogeneration plant is 38 percent lower compared to the conventional plant. This reduction in the irreversibility is accompanied by an increase in the thermal efficiency and utilization factor by 25 and 24 percent, respectively. The results show that the exergy destruction in the boiler is the highest.

Khalid Altayi [7] conducted an exergy and exergoeconomic analysis and a parametric study of a gas power plant, in response to the energy demand in Saudi Arabia. The conclusions of the assessment are as stated as followed:

- The combustion chamber has the highest exergy destruction, followed by the turbine.
- Increasing the exergetic efficiency results in reduced emissions, less environmental impact and enhanced sustainability
- Employing equations of conservation for mass, energy and exergy, a greater understanding of the system components as well as defining their efficiencies are achieved
- Showed that the combustion chamber has the highest exergy destruction, followed by the turbine. Additionally, he has demonstrated that by increasing the exergetic efficiency, the emissions will consequently be reduced, the environmental impact will be reduced and there will be a higher contribute for sustainability.

Yasin et al. [8] performed an exergy analysis of a turbofan engine for an unmanned aerial vehicle during a surveillance mission. The engine is the Rolls-Royce AE3007H, a high bypass turbofan engine and it was developed for the use on the Cessna Citation X. The results showed that the combustion chamber and the afterburner had the most exergy destruction within the engine. The study was well conducted, however, the modelling data from the engine may have incoherencies since the modelling it not demonstrated by the author and the only reference is that it was a result of comparing a genuine code with a modelling software. Additionally, some important thermodynamic parameters used in the exergy analysis, i.e. specific heat at constant pressure and enthalpy, may have been calculated using different formulas in comparison to the engine modelling.

Etele et al. [9] applied exergy analysis to a turbojet engine over flight altitudes ranging from sea level to 15 000m to define the reference selection effects. They concluded that the actual rational efficiency (defined as the ratio of useful work obtained from the system to the total quantity of the incoming exergy accounting for the incoming air and fuel) of this engine decreased with increasing altitude, varying from a value of 16.9% at sea level to 15.3% at 15 000 m.

3 Modelling the CFM56-5A1 Turbofan Engine

In order to conduct an exergetic analysis of an energy system, it is essential to create a mathematical model of the engine to obtain all basic quantities and properties (e.g., temperature, pressure, airflow). This chapter explains the methodology to conduct the modelling of the engine. The engine selected for the assessment was the CFM56-5A1 from CFMI manufacturer. After validation, the results were used to perform the exergy analysis in Chapter 5.

3.1 The CFM56-5A1 Engine

3.1.1 General Description

The CFM56-5A1 engine was developed in the first half of the 80's and entered in service in 1988. It was specially designed and optimized to power the short-to-medium range "150 passengers" Airbus A320 and later A319 aircraft [10]. It has a design bypass and overall pressure ratio of 6.0 and 26.5 its takeoff thrust ranges from 97.86 to 111.21 KN [12]. Currently, there are more than 1100 engines in service with more than 40 million flight hours.

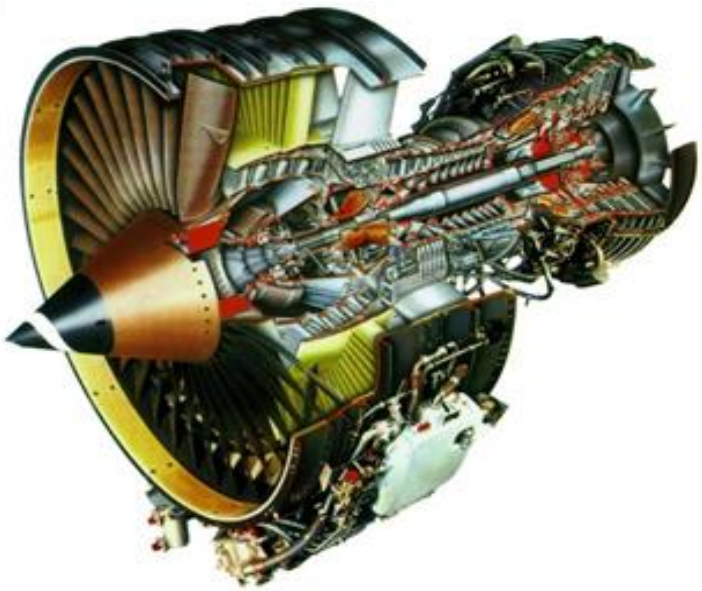

Figure 1: CFM56-5A1 engine [12]

The CFM56-5A1 engine is constituted by six main components:

- Fan
- Low Pressure Compressor (LPC)
- High Pressure Compressor (HPC)
- Combustion Chamber (CC)
- High Pressure Turbine (HPT)
- Low Pressure Turbine (LPT)

There are two drive shafts in this engine. The first connects the Fan and LPC to the LPT and constitutes de low pressure system. The second one connects the HPC to the HPT and constitutes the high pressure system. While the HPT runs the high pressure compressor, fuel pump, starter generator and reduction gearbox, the LPT runs the Fan and LPC.

This engine operates according to the Brayton Cycle, which includes four processes under the ideal conditions given below:

- Isentropic compression (Fan and HPC, 1-3)
- Combustion at constant pressure (CC, 3-4)
- Isentropic Expansion (HPT and LPT, 4-7)
- Heat transfer at constant pressure (Exhaust, 7-0)

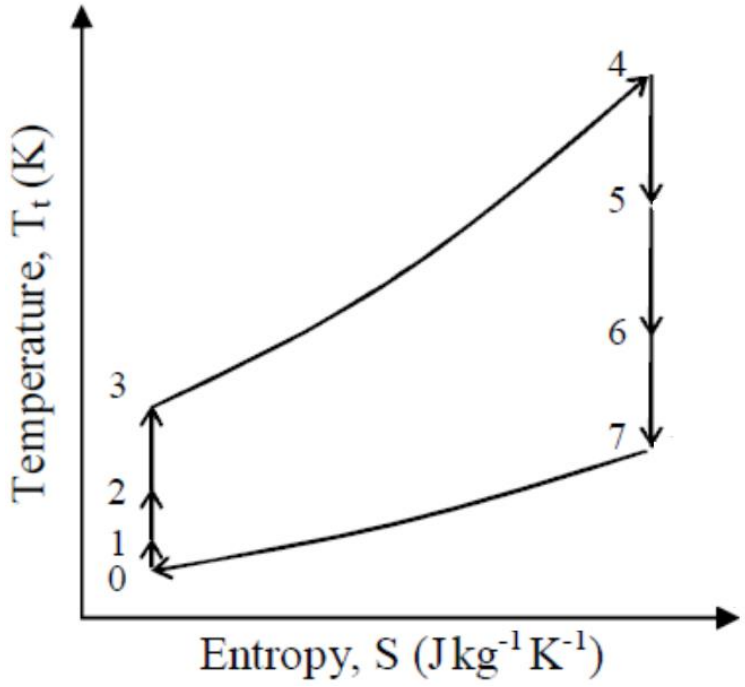

Figure 2: Brayton Cycle [12]

3.1.2 Technical Specifications

The CFM56-5A1 engine has the following specifications, obtained from references [11],[12],[14],[15]:

- Thrust (dry): 111.206 KN
- Thrust (cruise): 22.24 KN
- SFC (dry): 8.40 g/KN.s
- SFC (cruise): 15.1767 g/KN.s
- Airflow (static): 386.382 (Kg/s)
- OPR (static): 26.5
- BPR (static): 6.0
- FPR (takeoff): 1,55
- Cruise Speed (mach): 0.8
- Cruise Altitude: 10668 m
- Number of spools: 2
- Fan stages: 1
- LPC Stages: 3
- HPC Stages: 9
- HPT Stages: 1
- LPT Stages: 4
- Fan diameter: 1.73 m
- Engine Length: 2.42 m
- Width Diameter: 1.83 m

3.1.3 Engine Station Numbering

Due to the complexity of the engine and its components, a generalized schematic is shown in Figure 3.

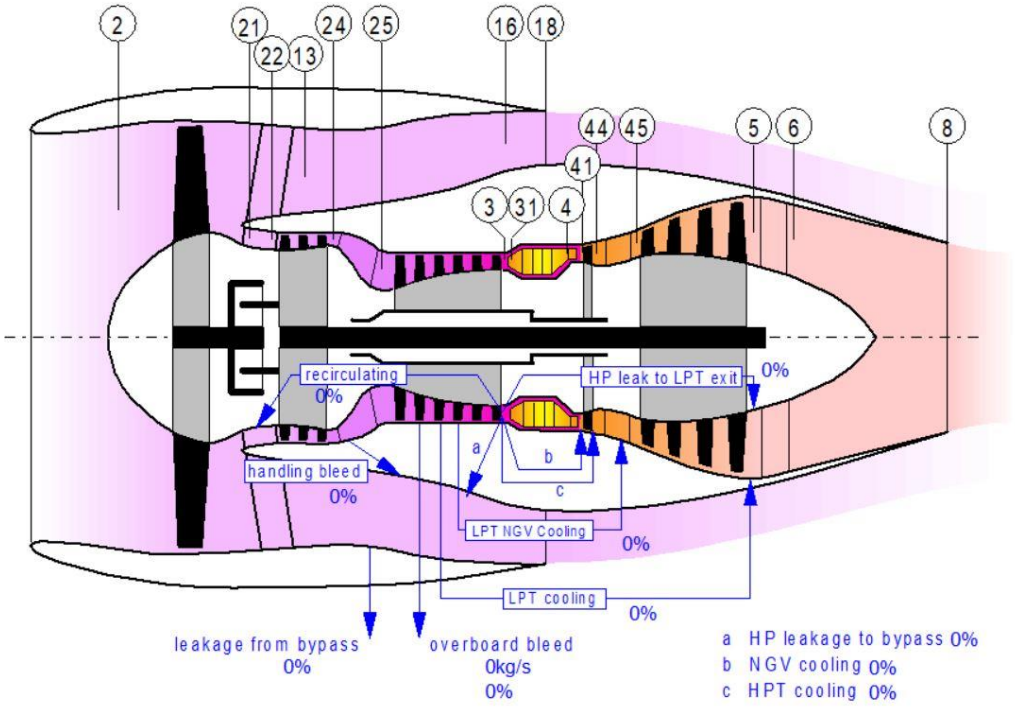

Figure 3: Engine components and stations, obtained from Gasturb software [16].

The indicated components and station numbers are listed in Table 1.

Table 1: Engine station numbering and their corresponding flows/locations.

Engine Station Number	Flow
13	Bypass Inlet Air
16	Bypass Medium Air
18	Bypass Outlet Air
2	Fan Inlet Air
21	Core Inlet Air
22	LPC Inlet Air
24	LPC Outlet Air
25	HPC Inlet Air
3	HPC Outlet Air
31	CC Inlet Air
4	CC Outlet Air
41	HPT Inlet Air
44	HPT Outlet Air
45	LPT Inlet Air
5/6	LPT Outlet Air
8	Nozzle Outlet Air

3.2 Modelling Conditions

To perform the modelling of the engine, it is important to clarify in which conditions the engine and the involving environment are being modelled.

Since the primary and longest flight phase is correspondingly the cruise, the engine was modelled for the cruise flight phase, as it is the most promising phase to perform the exergy analysis.

As for the ambient conditions, they were defined based on the typical cruise phase of the CFM56-5-A1, at 35000 feets (10668 metres). The conditions are listed on Table 2.

Table 2: Modelling Conditions.

Property	**Unit**	**Value**
Altitude	Meters	10668
Temperature	Kelvin	218.808
Mach		0.8

3.3 Matlab Modelling (Genuine Code)

This section presents the methodology used in the modelling of the engine with recourse to a genuine code. The methodology used to develop the genuine code is based on the process described by Walsh and Peter [17]. The code was built using the Matlab software.

3.3.1 Thermodynamic Fluid Properties

Since the thermodynamic fluid properties in a gas turbine have an enormous impact in its performance, it is essential that these gas properties are accounted rigorously in calculations, or that any inaccuracy due to simplifying assumptions is quantified and understood. Therefore, the following assumptions are made:

- The air flow through the engine is adiabatic.
- The engine is in a steady state, i.e. constant mass flow rate, fuel flow rate, thrust, inlet temperature, engine temperature distribution and engine speed.
- The air and combustion gases were assumed to be perfect gases.
- The component efficiencies are constant.

The most important thermodynamic properties to model a gas turbine are referred as follows [17]:

- Specific heat at constant pressure C_P and at constant volume C_V – defined as the amount of energy required to increase a unit mass of gas in 1ºC temperature at a constant pressure or volume respectively.
- Gas constant R – relates pressure and temperature changes and is numerically equal to the difference between C_P and C_V (simplified Mayer relation)
- Ratio of specific heats gamma γ – defined as the ratio of the heat capacity at constant pressure C_P to heat capacity at constant volume C_V.

To calculate the properties referred, the following formulas were considered [17]:

- Specific heat at constant pressure C_P for air before combustion:

$$C_P = A0 + A1 * TZ + A2 * TZ^2 + A3 * TZ^3 + A4 * TZ^4 + A5 * TZ^5 + A6 * TZ^6 + A7 * TZ^7 + A8 * TZ^8 \quad (1)$$

  Where $TZ = \frac{TS}{1000}$ and TS denotes for Static Temperature.

- Specific heat at constant pressure C_P for combustion products of kerosene in dry air:

$$C_P = A0 + A1 * TZ + A2 * TZ^2 + A3 * TZ^3 + A4 * TZ^4 + A5 * TZ^5 + A6 * TZ^6 + A7 * TZ^7 + A8 * TZ^8 + \left(\frac{FAR}{(1 + FAR)}\right) * (B0 + B1 * TZ + B2 * TZ^2 + B3 * TZ^3 + B4 * TZ^4 + B5 * TZ^5 + B6 * TZ^6 + B7 * TZ^7) \quad (2)$$

- Gas constant R for for products of combustion of kerosene in dry air:

$$R = 287.05 - 0.00990 * FAR + 10^{-6} * FAR^2 \quad (3)$$

- Adiabatic index γ:

$$\gamma = \frac{C_P}{C_P - R} \quad (4)$$

- Fuel-to-air ratio FAR:

$$FAR1 = 0.10118 + 2.00376 - 10^{-6} * (700 - T3) \quad (5)$$

$$FAR2 = 3.7078 * 10^{-3} - 5.2368 * 10^{-6} * (700 - T31) - 5.2632 * 10^{-6} * T4 \quad (6)$$

$$FAR3 = 8.889 * 10^{-8} * |(T4 - 950)| \quad (7)$$

$$FAR = (FAR1 - \sqrt{(FAR1^2 + FAR2)} - FAR3)/ETA34 \quad (8)$$

Where $ETA34$ is the combustion chamber efficiency, assumed to be 99%.

- Constants values for C_P calculation are listed in Table 3.

Table 3: Constants values for C_P calculation.

	Dry Air
A0	0.992313
A1	0.236688
A2	-1.852148
A3	6.083152
A4	-8.893933
A5	7.097112
A6	-3.234725
A7	0.794571
A8	-0.081873
A9	0.422178
A10	0.001053

As mentioned before, either Specific heat at constant pressure C_P, Gamma γ and Gas constant R are extensively used in engine performance calculations. According to Walsh and Fletcher [17], there are three methods for their calculation in each engine stage:

- Constant, standard values for C_P, and γ: this is used for classroom uses and crude estimates of component performance. It possesses an error of up to 5% [17]:
  - Cold end gas properties: C_P = 1004.7 J/kg K, γ = 1.4;
  - Hot end gas properties: C_P = 1156.9 J/kg K, γ = 1.33.

- Values based on mean temperatures: this iterative method is more accurate, and can be used both for dry air and combustion products of kerosene with an accuracy of 1.5% [17]. The mean temperature throughout the component is evaluated and C_P and γ are obtained from that value.
- Specific enthalpy and entropy: this method evaluates the enthalpy and entropy in the components, through polynomials of specific enthalpy and entropy obtained from the standard polynomials for specific heat. It is the most accurate, with 0.25% accuracy to all pressure ratios [17].

The method selected was the mean temperatures method, since it presents a high level of accuracy and is a viable method to implement. Despite the specific enthalpy and entropy method presented the best accuracy, it is complex to perform the calculations in respect to the available data.

3.3.2 Isentropic and Polytrophic efficiency

Despite not being thermodynamic fluid properties, it is also important to take in account the isentropic and polytrophic efficiency parameters.

Isentropic efficiency is, for the case of a power production device, the ideal specific power input, or total temperature rise (for constant mass flow rate and specific heats), divided by the actual for a given pressure ratio. It is a parameter to measure the degree of degradation of energy in steady-flow devices. It involves a comparison between the actual performance of a device and the performance that would be achieved under idealized circumstances for the same inlet and exit states. Isentropic means both adiabatic and reversible, which means it represent the efficiency of the process without heat transfer and friction.

Polytrophic efficiency is defined as the as the isentropic efficiency of an infinitesimally small step in the compression process, such that its magnitude would be constant throughout. It accounts for the fact that the inlet temperature of the stages of a compressor or turbine is not constant throughout the process of compression or expansion [17].

Therefore, polytrophic efficiency was used. However, for design point calculations, the isentropic efficiencies for the compressors and turbines had to be calculated, by using the following formulas [17]:

- Compressor isentropic efficiency

$$\eta_{c,isentropic} = \frac{PR^{\frac{\gamma-1}{\gamma}} - 1}{PR^{\frac{\gamma-1}{\gamma * \eta_{polytropic}}} - 1} \quad (9)$$

- Turbine isentropic efficiency

$$\eta_{t,isentropic} = \frac{1 - ER^{\frac{1-\gamma}{\gamma} * \eta_{polytropic}}}{1 - ER^{\frac{1-\gamma}{\gamma}}} \quad (10)$$

3.3.3 Methodology to model the engine

Considering the design point and ambient conditions referred in the last chapter, the following methodology to model the engine was considered:

- Intake

In the intake, there is an increase in the temperature and pressures values. The mass air flow $\dot{m}$ was taken from the specifications of the engine.

$$T_2 = T_0 * (1 + \frac{\gamma - 1}{2} * M^2) \quad (11)$$

$$P_2 = P_0 * \left(\frac{T_2}{T_0}\right)^{\frac{\gamma}{\gamma-1}} \quad (12)$$

$$\dot{m}_2 = \dot{m} \quad (13)$$

- Fan

After the intake, there is the fan compression stage. After the air flows through the fan, the flow divides in two, the core flow $\dot{m}_{21}$ that goes through the inner fan and the bypass flow $\dot{m}_{13}$ that goes through the outer fan. The core flow is considerably lower than the bypass flow due to the high bypass ratio. The inner fan and outer fan flow can be calculated by the following formulas:

$$\dot{m}_{21} = \frac{\dot{m}_2}{BR + 1} \quad (14)$$

$$\dot{m}_{13} = \dot{m}_2 - \dot{m}_{21} \quad (15)$$

The pressure increase was calculated by the following formulas:

$$P_{21} = P_2 * IFPR \quad (16)$$

$$P_{13} = P_{13} * OFPR \tag{17}$$

In this stage, the isentropic efficiencies for the inner fan $\eta_{if,isentropic}$ and outer fan $\eta_{of,isentropic}$ can be calculated by:

$$\eta_{isentropic,if} = \frac{IFPR^{\frac{\gamma-1}{\gamma}} - 1}{IFPR^{\frac{\gamma-1}{\gamma*\eta_{polytropic}}} - 1} \tag{18}$$

$$\eta_{isentropic,of} = \frac{OFPR^{\frac{\gamma-1}{\gamma}} - 1}{OFPR^{\frac{\gamma-1}{\gamma*\eta_{polytropic}}} - 1} \tag{19}$$

Next, the temperatures in the inner fan T_{21} and in the outer fan T_{13} were calculated:

$$T_{21} = \frac{T_2}{\eta_{isentropic,if}} * \left(OFPR^{\frac{\gamma-1}{\gamma}} - 1\right) + T_2 \tag{20}$$

$$T_{13} = \frac{T_2}{\eta_{isentropic,of}} * \left(IFPR^{\frac{\gamma-1}{\gamma}} - 1\right) + T_2 \tag{21}$$

At this step, it is fundamental to apply the mean temperature method described before:

$$T_m = \frac{T_{21} + T_2}{2} \tag{22}$$

$$T_m = \frac{T_{13} + T_2}{2} \tag{23}$$

After determining the first T_m, an iterative process starts to recalculate the new values for the C_P, γ and isentropic efficiency. The process stops when the following condition is achieved:

$$|T_{mean} - T_{mean}| \leq 0.00005 \tag{24}$$

When this condition is true, the last values of the iteration for T_{21} and T_{13} are chosen.

The power generated by the fan is then calculated by the following formula:

$$\dot{W}_{Fan} = \dot{m}_{21} * C_{P21mean} * (T_{21} - T_2) + \dot{m}_{13} * C_{P13mean} * (T_{13} - T_2) \tag{25}$$

- Bypass Duct

In this stage, the temperature and airflow remain constant but there is a slight pressure drop due to the expansion.

$$T_{18} = T_{13} \tag{26}$$

$$P_{18} = P_{13} * BDER \tag{27}$$

$$\dot{m}_{18} = \dot{m}_{13} \tag{28}$$

- Low Pressure Compressor

In this component, occurs the second compression stage. It is important to mention that the variations in temperature, pressure or airflow in the connection duct between the fan outlet and LPC inlet were neglected, therefore:

$$T_{22} = T_{21} \tag{29}$$

$$P_{22} = P_{21} \tag{30}$$

$$\dot{m}_{22} = \dot{m}_{21} \tag{31}$$

In this stage, it was used the mean temperature iterative method mentioned before to calculate T_{24}. The pressure increase, and the airflow remains constant.

$$T_{24} = \frac{T_{22}}{\eta_{isentropic,LPC}} * \left(LPCPR^{\frac{\gamma-1}{\gamma}} - 1\right) + T_{22} \tag{32}$$

$$P_{24} = P_{22} * LPCPR \tag{33}$$

$$\dot{m}_{24} = \dot{m}_{22} \tag{34}$$

The power generated by the LPC is calculated by the following formula:

$$\dot{W}_{LPC} = \dot{m}_{24} * C_{P24} * (T_{24} - T_{22}) \tag{35}$$

- High Pressure Compressor

In this component, occurs the third and last compression stage. The temperature and pressure remain constant between the LPC outlet and HPC inlet, therefore:

$$T_{25} = T_{24} \tag{36}$$

$$P_{25} = P_{24} \tag{37}$$

$$\dot{m}_{25} = \dot{m}_{24} \tag{38}$$

In this stage, it was used the mean temperature iterative method to calculate T_3. The temperature and pressure increase, and the airflow remains constant.

$$T_3 = \frac{T_{25}}{\eta_{isentropic,HPC}} * \left(HPCPR^{\frac{\gamma-1}{\gamma}} - 1\right) + T_{25} \tag{39}$$

$$P_3 = P_{25} * HPCPR \tag{40}$$

$$\dot{m}_3 = \dot{m}_{25} \tag{41}$$

The power generated by the HPC is calculated by the following formula:

$$\dot{W}_{HPC} = \dot{m}_3 * C_{P3mean} * (T_3 - T_{25}) \tag{42}$$

- Combustion Chamber

The temperature, pressure and flow remain constants between the HPC outlet and CC inlet, therefore:

$$T_{31} = T_3 \tag{43}$$

$$P_{31} = P_3 \tag{44}$$

$$\dot{m}_{31} = \dot{m}_3 \tag{45}$$

In this component, occurs the combustion process with injection of fuel into the CC. The fuel flow and the total mass flow is calculated by the following equations:

$$\dot{m}_{fuel} = \dot{m}_{31} * FAR \quad (46)$$

$$\dot{m}_4 = \dot{m}_{31} + \dot{m}_{fuel} \quad (47)$$

The outlet pressure is calculated using the BDE [11]:

$$P_4 = P_{31} * BDE \quad (48)$$

The CC outlet temperature T_4 was obtained from [15].

- High Pressure Turbine:

The temperature, pressure and flow remain constants between the CC outlet and HPT inlet, therefore:

$$T_{41} = T_4 \quad (49)$$

$$P_{41} = P_4 \quad (50)$$

$$\dot{m}_{41} = \dot{m}_4 \quad (51)$$

In this component, occurs the first expansion stage. The expansion stages require a different approach to calculate the objective parameters. The first step is to calculate the power generated by the HPC. Therefore, it was used the following formula:

$$\dot{W}_{HPT} = \frac{\dot{W}_{HPC}}{\eta_{HPS}} \quad (52)$$

The temperature is calculated by the following formula:

$$T_{44} = T_{41} - \frac{\dot{W}_{HPT}}{\dot{W}_{41} * C_{P41}} \quad (53)$$

In order to calculate the pressure, a new iterative method was created, since the expansion ratio is unknown. First, the isentropic efficiency is calculated, assuming an acceptable value for the HPTER equal to 4.

$$\eta_{t,isentropic} = \frac{1-HPTER^{\frac{1-\gamma}{\gamma}*\eta_{polytropic}}}{1-HPTER^{\frac{1-\gamma}{\gamma}}} \quad (54)$$

The isentropic efficiency is used to obtain the expansion ratio.

$$HPTER = \left(\frac{1}{1 - \frac{T_{41} - T_{44}}{\eta_{t,isentropic}} * T_{41}} \right)^{\frac{\gamma-1}{\gamma}} \quad (55)$$

The iterative process restarts until the following condition is achieved:

$$\left| HPTER - HPTER_{previous} \right| \leq 0.00005 \quad (56)$$

When this condition is true, the last value of the iteration is chosen.

The pressure is calculated by the following formula:

$$P_{44} = \frac{P_{41}}{HPTER} \quad (57)$$

The airflow in this stage remains constant:

$$\dot{m}_{44} = \dot{m}_{41} \quad (58)$$

- Low Pressure Turbine:

The temperature, pressure and flow remain constants between the HPT outlet and LPT inlet, therefore:

$$T_{45} = T_{44} \quad (59)$$

$$P_{45} = P_{44} \quad (60)$$

$$\dot{m}_{45} = \dot{m}_{44} \quad (61)$$

In this component, occurs the second expansion stage. It was used the same method referred in the HPC methodology to calculate the objective parameters. The power generated is written as follows:

$$\dot{W}_{LPT} = \frac{\dot{W}_{LPC} + \dot{W}_{Fan}}{\eta_{LPS}} \tag{62}$$

The temperature is calculated by the following formula:

$$T_5 = T_{45} - \frac{\dot{W}_{LPT}}{\dot{W}_{45} * C_{P45}} \tag{63}$$

To calculate the pressure, it was used the same iterative method as referred before. The resultant value achieved in the iteration for the LPTER is used in the following formula:

$$P_5 = \frac{P_{45}}{LPTER} \tag{64}$$

The airflow in this stage remains constant:

$$\dot{m}_5 = \dot{m}_{45} \tag{65}$$

- Exhaust Nozzle:

The airflow and temperature remain constant, although there is a slight pressure drop:

$$\dot{m}_8 = \dot{m}_5 \tag{66}$$

$$T_8 = T_5 \tag{67}$$

$$P_8 = P_5 * NE \tag{68}$$

- Thrust and TSFC

To calculate these parameters, it is essential to determine the hot nozzle thrust, Th_{hot}, and the cold nozzle thrust, Th_{cold}. The following approach was considered:

$$M_8 = \sqrt{\frac{2}{\gamma-1} * \left(\frac{P_8}{P_0}^{\frac{\gamma-1}{\gamma}} - 1\right)} \tag{69}$$

$$T_{8s} = \frac{T_8}{1+\frac{\gamma-1}{8} * {M_8}^2} \tag{70}$$

$$Q = 1000 * \sqrt{\frac{2*\gamma}{(\gamma-1)*R} * \frac{P_8}{P_0}^{-\frac{2}{\gamma}} * (1 - \frac{P_8}{P_0}^{-\frac{1-\gamma}{\gamma}})} \quad (71)$$

$$P_{8s} = \frac{P_8}{\frac{T_8}{T_{8s}}^{\frac{\gamma}{\gamma-1}}} \quad (72)$$

$$A_{effect,hot} = \frac{\dot{m}_8 * \sqrt{T_8}}{Q * P_8} \quad (73)$$

$$a_8 = \sqrt{\gamma * R * T_{8s}} \quad (74)$$

$$v_8 = a_8 * M_8 \quad (75)$$

$$Th_{hot} = \dot{m}_8 * v_8 + A_{effect,hot} * (P_{8s} - P_{amb}) \quad (76)$$

This method is applicable to the hot thrust. For the cold thrust, it was used the same method, but using the station 18, corresponding to the bypass duct outlet.

To calculate the net thrust and TSFC, the following formulas were considered:

$$Th_{net} = Th_{hot} + Th_{cold} \quad (77)$$

$$TSFC = \frac{\dot{m}_{fuel}}{Th_{net}} \quad (78)$$

3.3.4 Modelling Results

The results obtained are presented in Tab.4 and Tab.5.

Table 4: Airflow, temperature, and pressure results.

Station	$\dot{m}$	T	P
	[Kg/s]	[K]	[kPa]
0	----	218.8100	23.842
2	149.00	246.8177	36.343
13	127.71	283.5827	56.332
21	21.28	283.3103	56.332
22	21.28	283.3103	56.332
24	21.28	481.0968	313.206
25	21.28	481.0968	313.206
3	21.28	801.4569	1741.429

31	21.28	801.45	1741.429
4	21.73	1538.15	1645.360
41	21.73	1538.15	1645.360
44	21.73	1274.03	648.034
45	21.73	1274.03	648.034
5	21.73	906.27	124.335
6	21.73	906.27	124.335
8	21.73	906.27	123.201
18	127.71	283.58	55.899

Table 5: Thrust and TSFC obtained from the modelling.

Th [kN]	**TSFC** [g/kN.s]
26.53	16.47

3.4 Gasturb 13 Modelling

3.4.1 Software Description

With the intention of having a comparison measure in respect with the modelling performed before and to verify its results, an additional modelling was performed using the professional software Gasturb 13. This software was developed to study energy systems using gas turbines and it is useful for those working for gas turbine industry, airframe manufactures and airlines, engine maintenance companies and operators of air, land and sea based gas turbines. With this software, users can evaluate easily the thermodynamic cycle of the most common gas turbine architectures, both for engine on-design and off- design conditions.

3.4.2 Methodology to model the engine

The first step for modelling an engine with this software is to choose which type of engine is going to be studied. In Figure 4, it is shown the Gasturb menu with diverse types of engines.

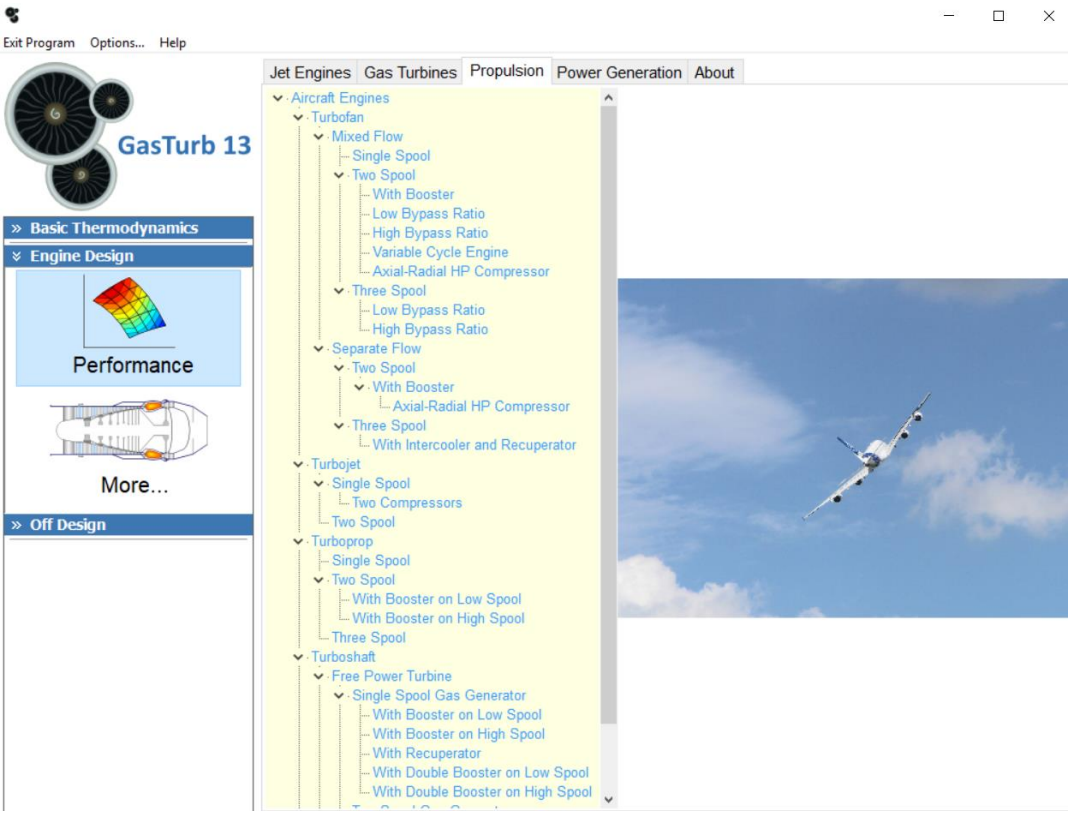

Figure 4: Gasturb engine selection menu.

The author chose the turbofan engine with two spools, unmixed flows and with booster. This engine has the same configuration of the CFM56-5A1.

The second step is to choose the scope of the analysis and the calculation mode. There are two scopes of analysis: the “Basics Thermodynamics” and “Performance”. The author chose the “Performance”, since that the user is able to insert more complex data, i.e. engine efficiencies, exhaust nozzle calculations and others. The calculation mode chose was the “on design”.

In the third and last step, the software requires several inputs parameters introduced by the user. Those are the ambient conditions and the engine data provided by the manufacturer. It is important to mention that, due to product secrecy policies, the available data to model the engine is limited. The ambient conditions are stated on section 3.2 and the engine data required are referred as follows:

- Overboard bleed
- Burner exit temperature
- Bypass Ratio
- Components efficiencies
- Compressor pressure ratios
- Total mass flow

The overboard bleed was assumed to be shut off, as there are no data available and trying to iterate it could cause errors in the results. The burner exit temperature was obtained from reference [15]. The bypass ratio, compressor pressure ratios and total mass flow were obtained from reference [11]. The components efficiencies were assumed as the standard values provided by the software. These efficiencies were used also in the first modelling. The engine operates with Jet-A1, also referred as Kerosene, and its fuel heating value was obtained from reference [15]. Table 6 presents the inputs required to be inserted in the software.

Table 6: Gasturb modelling inputs.

Intake Pressure Ratio		1
No (0) or Average (1) Core dP/P		1
Inner Fan Pressure Ratio		1,55
Outer Fan Pressure Ratio		1,55
Core Inlet Duct Press. Ratio		1
IP Compressor Pressure Ratio		5,56
Compressor Interduct Pressure Ratio		1
HP Compressor Pressure Ratio		5,56
Bypass Duct Pressure Ratio		0,992322
Turbine Interduct Pressure Ratio		1
Design Bypass Ratio		6
Burner Exit Temperature	K	1538,15
Burner Design Efficiency		1
Burner Partload Constant		1
Fuel Heating Value	MJ/kg	42,8
Overboard Bleed	kg/s	0
Power Offtake	kW	0
HP Spool Mechanical Efficiency		1
Gear Ratio		2,5
LP Spool Mechanical Efficiency		1
Burner Pressure Ratio		0,95
Turbine Exit Duct Press Ratio		1

When a modelling of an engine is done with limited data, it is important to understand if the final results obtained are in accordance with the expected engine real performance. Therefore, there are two main goals to achieve a correct modelling of the engine. The TSFC and the thrust generated must be in agreement with the engine real performance for a specific operating mode. In this case, the TSFC and thrust for the cruise flight must be equal to those specified by the manufacturer, also for cruise flight. Figure 5 reflects the workflow to achieve a correct modelling. If the TSFC and Thrust results are not the expected, the engine data must be iterated, in respect to its normal limits, to reach to the correct values.

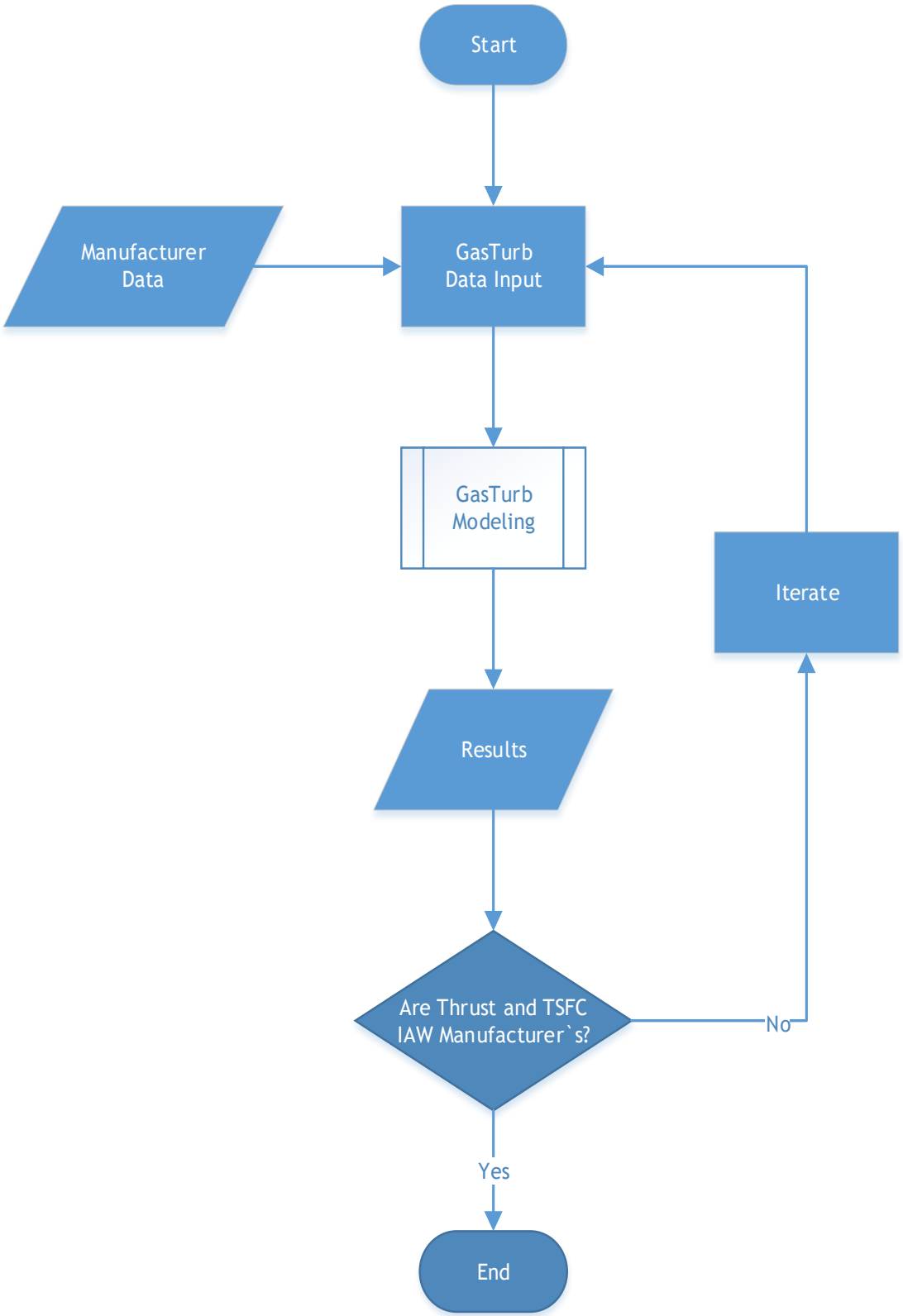

Figure 5: Gasturb modelling workflow.

3.4.3 Modelling Results

The results obtained are presented in Table 7 and Table 8.

Table 7: Airflow, temperature, and pressure obtained from the modelling.

Station	$\dot{m}$	T	P
	[Kg/s]	[K]	[kPa]
0	----	218.81	23.842
2	149.62	246.88	36.354
13	128.24	283.62	56.349
21	21.37	283.35	56.349
22	21.37	283.35	56.349
24	21.37	480.86	313.299
25	21.37	480.86	313.299
3	21.37	802.10	1741.942
31	21.37	802.10	1741.942
4	21.84	1538.15	1654.845
41	21.84	1538.15	1654.845
44	21.84	1270.76	651.676
45	21.84	1270.76	651.676
5	21.84	896.14	125.023
6	21.84	896.14	125.023
8	21.84	896.14	125.023
18	128.24	283.62	55.916

Table 8: Thrust and TSFC obtained from the modelling.

Th [kN]	**TSFC** [g/kN.s]
27.2901	17.1535

3.5 Validation

The Matlab simulation results were analysed and compared with the Gasturb results. The Matlab script until the CC stage, has a very high accuracy since the maximum variation is inferior to 1%. In the turbine stages, the Matlab script has a lower accuracy since the maximum variation is around 10%. This loss of accuracy occurs do to the fact that the Gasturb uses the method of enthalpy and polynomials while in the script it was used the mean temperature method.

Comparing the thrust generated and TSFC of the Matlab script with the Gasturb, the variation is inferior to 1%. Comparing the refered Matlab results with the manufacturer`s specifications, there is a variation of 17% in the thrust generated. It is acceptable, since both simulations, where made without considering the overboard bleeds.

Despite the small loss of accuracy, the Matlab results are in accordance with the expected and are considered acceptable, therefore, those were selected for the exergy analysis.

4 Exergy Fundamentals

4.1 Introduction

Exergy can be defined as the maximum available work that can be produced by an energy system as it comes to equilibrium with its reference environment. Exergy analysis is based in the fact that every energy system that is not in equilibrium with its reference environment, can produce work, and when it is in equilibrium, it has zero exergy since it has no capability to do work with respect to its reference environment. It also acknowledges that, although exergy cannot be created or destroyed, it can be degraded in quality, eventually reaching a state in which it is in complete equilibrium with the surroundings and hence of no further use for performing.

Exergy is often called available energy, availability, work capability, essergy, and so forth. Exergy is not a thermodynamic quantity, but it depends on thermodynamic quantities (i.e. enthalpy, entropy and others).

Exergy analysis combines both First and Second Law of thermodynamics. This method uses the conservation of energy principles, together with the second law of thermodynamics. It is a tool that "measures" the quality of the energy. It provides a true measure of how nearly actual performance of an energy system approaches the ideal.

The primary goal of exergy analysis is to identify and minimize the irreversibilities on each component of an energy system. It is useful to improve the performance and build more efficient energy systems, since it can identify and calculate the locations, types, and true magnitudes of wastes and destruction of exergy.

In general, more meaningful efficiencies are evaluated with exergy analysis than with energy analysis, since exergy efficiencies are always a measure of the approach to the ideal. Therefore, exergy analysis identifies accurately the margin available to design more efficient energy systems by reducing inefficiencies. Many engineers and scientists suggest that thermodynamic performance is best evaluated using exergy analysis because it provides more insights and is more useful in efficiency improvement efforts than energy analysis [18].

4.2 Why Exergy Analysis?

Exergy analysis brings some huge importance and benefits, for studying and assessing energy systems, because of the following facts:

- It improves designs and provides better analysis by combining both first and second laws of thermodynamics.
- It improves the efficiency of energy by identifying efficiencies that always measure the approach to ideality as well as the location, types, and true magnitudes.
- It reveals if and by how much it is possible to design more efficient systems by reducing the energy losses in existing systems.
- It's capable of measuring the impact on the environment of energy and other resource utilization, and reducing or mitigating that impact.
- Identifying whether a system contributes to achieving sustainable development or is unsustainable.

4.3 Exergy Characteristics

As referred before, exergy analysis provides great benefits in respect of assessing energy systems. The most relevant characteristics of exergy are referred as follows [3]:

- If a system is at its dead state (in equilibrium with the reference environment), it has zero exergy, since there are no differences in temperature, pressure, concentration, and consequently, no processes can be triggered.
- The exergy increases the more the parameters of the system and the environment diverges from each other. As an example, a block of ice has a higher exergy in a hot environment than in a cold one.
- Exergy, by definition, depends not only on the state of a system but as well as the state of the reference environment.
- When energy loses its quality, exergy is destroyed. Exergy is the part of energy that is useful, therefore, it has economic value, so it is worth managing it well.
- Energy resources with high exergy contents are usually more valued than energy resources with low exergy contents. As an example, fossil fuels have high energy and energy contents. Contrasting with this, waste heat has high energy, but low exergy, therefore it has a limited value.

4.4 Exergy Components

Considering the non-existence of nuclear, magnetic, electrical or surface tension effects, the exergy can be divided in four components (Figure 6):

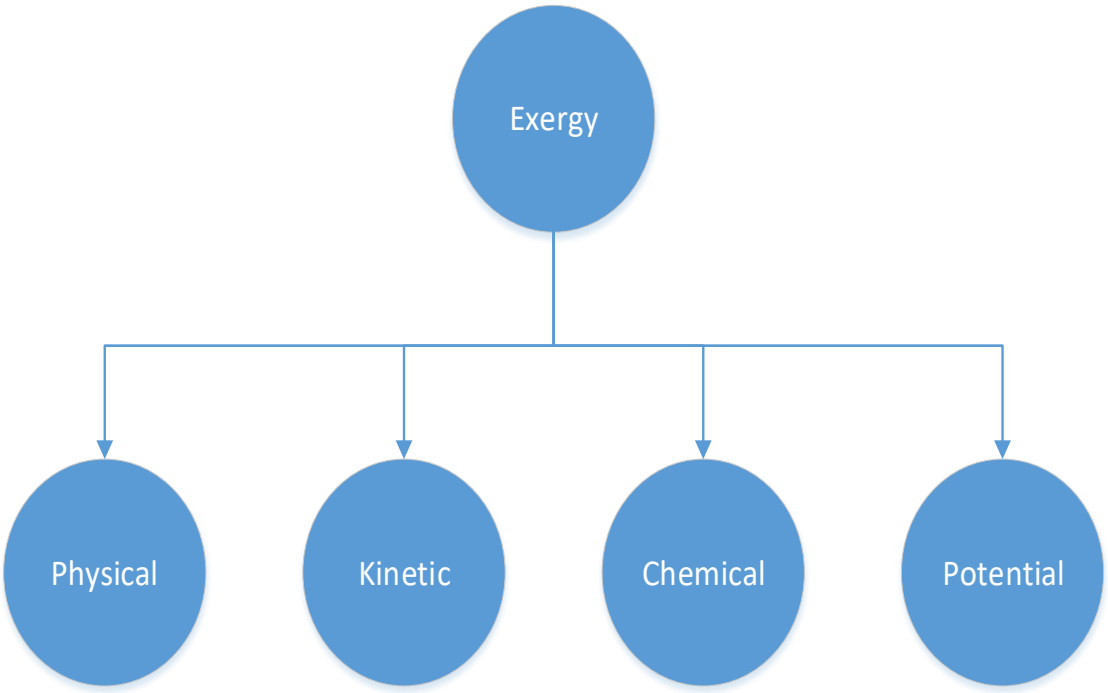

Figure 6: Exergy components.

Physical exergy is defined as the maximum amount of work obtainable from a system as its temperature and pressure are brought to equal values of those in the reference environment.

Kinetic exergy is equal to the kinetic energy itself regardless of the temperature and pressure of the environment.

Chemical exergy is defined as the maximum amount of work that can be obtained when a substance is brought from the reference environment state to the dead state by a process including heat transfer and exchange of substances only with the reference environment. Alternatively, chemical exergy can also be viewed as the exergy of a substance that is at the reference-environment state.

Potential exergy is equal to the potential energy itself and does not depend on pressure and temperature.

The total exergy of the system is composed by the sum of all components referred before. It can be written as follows [19]:

$$E = E^{PH} + E^{KN} + E^{CH} + E^{PT} \tag{79}$$

Considering any steady state system, for a control volume, which $\dot{m}$ denotes for mass flow rate, the total exergy of a system can be written as follows [8]:

$$\dot{E} = \dot{m}(e^{PH} + e^{KN} + e^{CH} + e^{PT}) \quad (80)$$

Since the turbofan engine was modelled in the cruise flight phase, i.e. at constant air speed and altitude, kinetic and potential exergy were not considered for the exergy analysis.

4.5 Physical Exergy

Physical exergy or flow exergy, as referred before, is the maximum useful work obtainable by taking the substance through reversible process from its initial state (T, P) to the state of the reference environment (T_0, P_0). Since kinetic and potential energy are not taken into consideration, the physical exergy e^{PH} can be determined with the enthalpy and entropy values of the stream at a given temperature and pressure, and the reference environmental state temperature (T_0) and pressure (P_0). Therefore, the specific physical exergy e^{PH} of a stream or flow can be written as follows [3]:

$$e^{PH} = (h - h_0) - T_0(s - s_0) \quad (81)$$

The terms of h and s denotes for specific enthalpy and entropy respectively. If the gas flow is assumed to be ideal, and assuming a constant specific heat, equation (81) can be written as follows [8]:

$$e^{PH} = C_p(T - T_0) - T_0\left[C_p \ln\left(\frac{\mathrm{T}}{T_0}\right) - R \ln\left(\frac{P}{P_0}\right)\right] \quad (82)$$

4.6 Chemical Exergy

The chemical exergy is the maximum work extractable as the system that is already in thermal and mechanical equilibrium with the reference environment, is brought into chemical equilibrium with the reference environment. By other words, chemical exergy can be defined as the theoretical maximum useful work that can be obtained when a substance is brought from the reference environment state to the dead state by a process including heat transfer and exchange of substances only with the reference environment.

Chemical exergy can be divided in two parts (Figure 7):

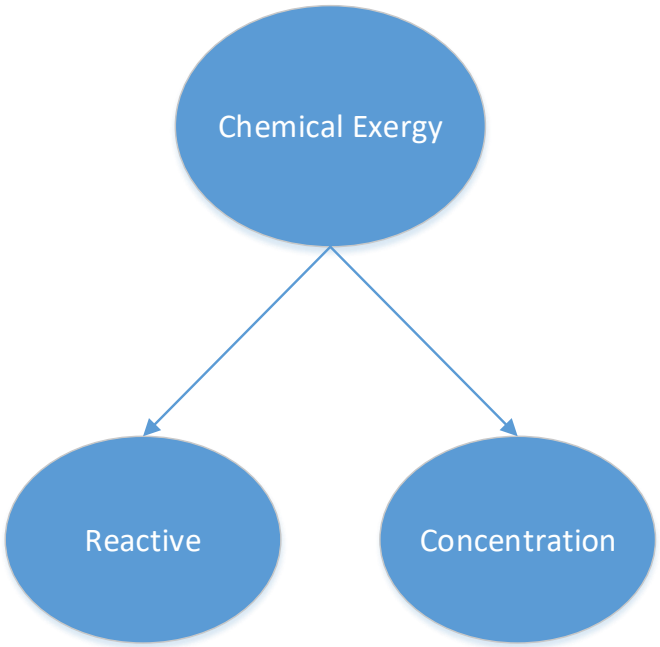

Figure 7: Chemical exergy components.

The reactive exergy is the corresponding exergy resulted from chemical reactions, to generate species that do not exist as stable components in the reference environment.

The concentration exergy is the exergy resulting from the different chemical concentrations of the species present in the energy system and in the reference environment. In addition, it is related to the exergy of purifying or diluting a substance.

The specific chemical exergy of an ideal gas mixture can be expressed as follows [8]:

$$\bar{e}_{mix}^{CH} = \sum_{i=1}^{n} X_i \bar{e}_i^{CH} + RT_0 \sum_{i=1}^{n} X_i \ln(X_i) + G^E \tag{83}$$

The X_i and e_i^{CH} denote the mole fraction and standard chemical exergy of each mixture component respectively. The term G^E denotes for Gibbs free energy, which is a negligible quantity in a gas mixture operated at low pressure. This formula is applicable if the energy system conditions don't vary too much in respect with the reference environment. For other cases, a different formula can be expressed as follows [4]:

$$\bar{e}_{mix}^{CH} = T_0 R \sum_{i=1}^{n} \lambda_i X_i \ln\left(\frac{X_i}{X_i^e}\right) \tag{84}$$

The λ_i and X_i^e denote the mass fraction of the constituent and the mole fraction of the constituent in the reference environment.

The standard chemical exergy for the main constituents of air are listed in Table 9 [3].

Table 9: Standard chemical exergy of air constituents.

Air Constituents	**Formula**	$\bar{e}_i^{CH}$(kJ/mol)
Nitrogen	N_2	0.72
Oxygen	O_2	3.97
Water	H_2O	9.49
Argon	Ar	11.69
Carbon dioxide	CO_2	19.87
Hydrogen	H_2	236.1

4.7 Fuel exergy

The fuel exergy is a particular case of the chemical exergy. It can be defined as the extractable work between the state of unburned fuel and the state on which the burned fuel and the reference environment are in complete equilibrium with each other.

To determinate the chemical exergy of fuels, an exergy to energy ratio equation can be used. The chemical exergy of a fuel, can be defined as follows [4]:

$$e_{fuel}^{CH} = \phi LHV \tag{85}$$

The LHV denotes for low heating value of the fuel and ϕ denotes for the ratio of fuel exergy to lower heating value. For most of gaseous fuels, the value of ϕ is normally close to 1. For a liquid fuel with composition$(C_\alpha H_\beta N_\gamma O_\delta)$, based on their atomic composition, the ratio of fuel exergy to lower heating value can be written as follows [3]:

$$\phi = 1.0401 + 0.1728\frac{\beta}{\alpha} + 0.0432\frac{\delta}{\alpha} + 0.2169\frac{\gamma}{\alpha}\left(1 - 2.062\frac{\beta}{\alpha}\right) \tag{86}$$

The accuracy of this equation is estimated as ±0.38% [20].

The turbofan engine operates with Jet-A1 fuel, also referred as kerosene. Its chemical formula and LHV are $C_{12}H_{23}$ and 42800 kJ/kg respectively [16].

4.8 Reference Environment

As the exergy of an energy system is determined according to its environment, it is important to define a suitable reference environment. The reference environment is a large equilibrium system in which the state variables (T_0, P_0) and the chemical potential of the chemical components contained in it remain constant, when in a thermodynamic process heat and materials are exchanged between another system and the environment. No chemical reactions can occur between the environment components. Despite the fact of the environment being a huge complex system with numerous chemical substances, it is normally modelled with the primary and most present substances of the atmosphere.

It is also important to mention that the chosen reference environment should agree with the ambient conditions the energy system usually operate, in this case, with the modelling ambient conditions of the engine. Therefore, the reference environment state variables and composition were chosen, in accordance with the engine modelling conditions and are listed in Table 10 [21] .

Table 10: Atmosphere composition.

Air Constituents	**Formula**	**Molar** Fraction
Nitrogen	N_2	0.7567
Oxygen	O_2	0.2035
Water	H_2O	0.0303
Argon	Ar	0.0091
Carbon dioxide	CO_2	0.0003
Hydrogen	H_2	0.0001

4.9 Dead State

An energy system is at the dead state when it is in thermal, mechanical and chemical equilibrium with the reference environment. At the dead state, a system:

- Is at the temperature and pressure of its environment.
- It has no kinetic or potential energy relative to the environment (zero velocity and zero elevation above a reference level).
- Does not react with the reference environment since they achieve the same chemical composition (chemically inert).

If these conditions are achieved, the system cannot suffer any change by any form of interaction with the environment. Additionally, there are no unbalanced magnetic, electrical, and surface

tension effects between the system and its surroundings, if these are relevant to the situation at hand.

4.10 Figures of Merit

In order to perform an exergetic assessment, performance parameters must be taken in account to evaluate an energy system and its components. These are the exergy efficiency; improvement potential; relative exergy destruction rate; fuel depletion rate and productivity lack. Those were consulted on references [4],[8],[18],[19],[22].

The exergy efficiency ε is defined as the ratio between exergy rates of product $\dot{E}_P$ and fuel $\dot{E}_F$. The product exergy represents the desired result produced and the fuel exergy represents the resources used to generate the product:

$$\varepsilon = \frac{\dot{E}_P}{\dot{E}_F} \tag{87}$$

The improvement potential $\dot{IP}$ is defined as the rate of exergy destruction within the system. It measures the margin available to improve and reduce irreversibilites:

$$\dot{IP} = \dot{E}_D(1 - \varepsilon) \tag{88}$$

The relative exergy destruction χ is defined as the ratio of the exergy destruction rate of a component to the total exergy destruction rate of a system. It indicates the percentage of exergy destruction within the system. It is written as follows:

$$\chi = \frac{\dot{E}_D}{\sum \dot{E}_D} \tag{89}$$

The fuel depletion rate δ is defined as the ratio of the exergy destruction rate to the total fuel exergy rate entering in the system:

$$\delta = \frac{\dot{E}_D}{\sum \dot{E}_F} \tag{90}$$

The productivity lack ξ is the ratio of exergy destruction rate to total exergetic product rate within the system. It indicates the product loss in the form of exergy destruction or shows how much product exergy potential is lost due to exergy destructions. It is written as follows:

$$\xi = \frac{\dot{E}_D}{\sum \dot{E}_P} \tag{91}$$

5 Exergy Analysis

5.1 Assumptions

In this exergy analysis, the assumptions made are as follows:

- The engine was considered under steady-state conditions at cruise flight conditions.
- The air and combustion gases were assumed to be perfect gases.
- The chosen fuel was kerosene (Jet-A1). The chemical formula of the kerosene considered was $C_{12}H_{23}$, while the low heating value of the kerosene was 42800 kJ/kg.
- The combustion reaction was considered completed.
- The kinetic and potential exergies were not considered for this analysis.
- The bleed air system was assumed to be shut off.

5.2 Combustion Modelling

For the purpose of calculating the chemical exergy within the engine, the combustion must be modelled to calculate the composition of the air inside the engine, after the combustion stage. The chemical equation of the combustion process of a hydrocarbon fuel in air can be expressed as follows [23]:

$$C_\alpha H_\beta + \left(\alpha + \frac{1}{4}\beta\right)(O_2 + 3.76N_2) \rightarrow \alpha CO_2 + \frac{\beta}{2}H_2O + 3.76\left(\alpha + \frac{\beta}{4}\right)N_2 \quad (92)$$

By applying the kerosene chemical formula $C_{12}H_{23}$, the equation (92) can be written as follows:

$$C_{12}H_{23} + (17.75)(O_2 + 3.76N_2) \rightarrow 12CO_2 + 11.5H_2O + 17.75(3.76)N_2 \quad (93)$$

The molar fraction of the resulting combustion products can be calculated by the following formulas [24]:

$$\gamma_{CO_2} = \frac{\alpha}{4.76\left(\alpha + \frac{\beta}{4}\right) + \frac{\beta}{4}} \quad (94)$$

$$\gamma_{H_2O} = \frac{\frac{\beta}{2}}{4.76\left(\alpha + \frac{\beta}{4}\right) + \frac{\beta}{4}} \quad (95)$$

$$\gamma_{N_2} = \frac{3.76\left(\alpha + \frac{\beta}{4}\right)}{4.76\left(\alpha + \frac{\beta}{4}\right) + \frac{\beta}{4}} \tag{96}$$

The molar fraction of the combustion gases was obtained as 0.1330 for CO_2, 0.1274 for H_2O, 0.7396 for N_2.

5.3 Governing Equations

The general mass balance, energy balance, exergy balance equations are stated as follows:

- Mass balance:

$$\sum \dot{m}_{in} = \sum \dot{m}_{out} \tag{97}$$

Where $\dot{m}$ is the mass flow rate, and subscript in and out denote for inlet and outlet of the system, respectively.

- Energy balance:

$$\sum \dot{m}_{in} h_{in} + \sum \dot{W}_{in} = \sum \dot{m}_{out} h_{out} + \sum \dot{W}_{out} \tag{98}$$

Where h and $\dot{W}$ denote for total enthalpy and work rate, respectively.

- Exergy balance:

$$\sum \dot{E}_{in} - \sum \dot{E}_{out} = \sum \dot{E}_{dest} \tag{99}$$

Where $\dot{E}$ and the subscript $dest$ denote for total exergy and destroyed, respectively.

Next, the referred equations and the figures of merit are applied and presented to each component of the engine. Additionally, the exergy flows are also represented in Figures 8, 9, 10, 11, 12 and 13.

➢ Fan

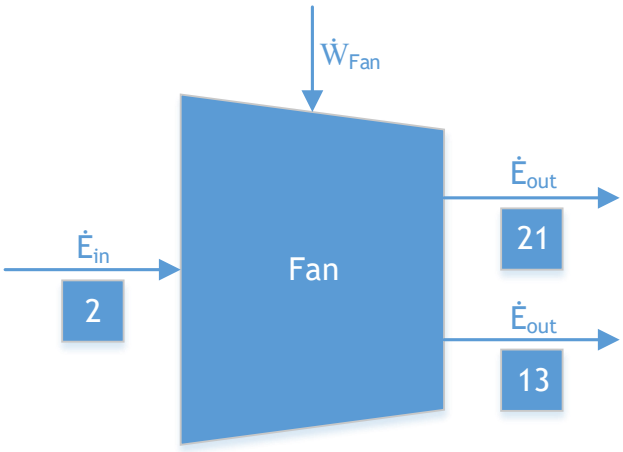

Figure 8: Exergy flows in the fan.

$$\dot{m}_2 = \dot{m}_{21} + \dot{m}_{13} \tag{100}$$

$$-\dot{w}_{Fan} + \dot{m}_2 h_2 - \dot{m}_{21} h_{21} - \dot{m}_{13} h_{13} = 0 \tag{101}$$

$$\dot{w}_{Fan} + \dot{E}_2 - \dot{E}_{21} - \dot{E}_{13} - \dot{E}_{D,Fan} = 0 \tag{102}$$

$$\varepsilon_{Fan} = \frac{\dot{E}_{21} + \dot{E}_{13} - \dot{E}_2}{\dot{w}_{Fan}} \tag{103}$$

$$I\dot{P}_{Fan} = \dot{E}_{D,Fan}(1 - \varepsilon_{Fan}) \tag{104}$$

$$\chi_{Fan} = \frac{\dot{E}_{D,Fan}}{\sum \dot{E}_D} \tag{105}$$

$$\delta_{Fan} = \frac{\dot{E}_{D,Fan}}{\sum \dot{E}_F} \tag{106}$$

$$\xi_{Fan} = \frac{\dot{E}_{D,Fan}}{\sum \dot{E}_P} \tag{107}$$

- Low Pressure Compressor

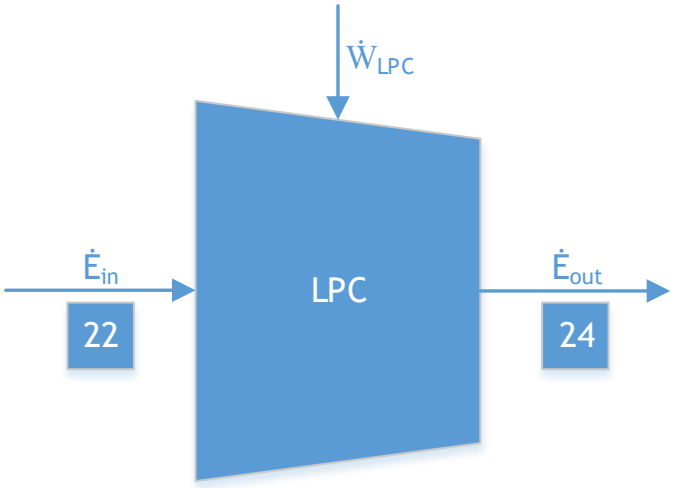

Figure 9: Exergy flows in the LPC.

$$\dot{m}_{22} = \dot{m}_{24} \tag{108}$$

$$-\dot{w}_{LPC} + \dot{m}_{22}h_{22} - \dot{m}_{24}h_{24} = 0 \tag{109}$$

$$\dot{w}_{LPC} + \dot{E}_{22} - \dot{E}_{24} - \dot{E}_{D,LPC} = 0 \tag{110}$$

$$\varepsilon_{LPC} = \frac{\dot{E}_{24} - \dot{E}_{22}}{\dot{w}_{LPC}} \tag{111}$$

$$\dot{IP}_{LPC} = \dot{E}_{D,LPC}(1 - \varepsilon_{LPC}) \tag{112}$$

$$\chi_{LPC} = \frac{\dot{E}_{D,LPC}}{\sum \dot{E}_D} \tag{113}$$

$$\delta_{LPC} = \frac{\dot{E}_{D,LPC}}{\sum \dot{E}_F} \tag{114}$$

$$\xi_{LPC} = \frac{\dot{E}_{D,LPC}}{\sum \dot{E}_P} \tag{115}$$

➢ High Pressure Compressor

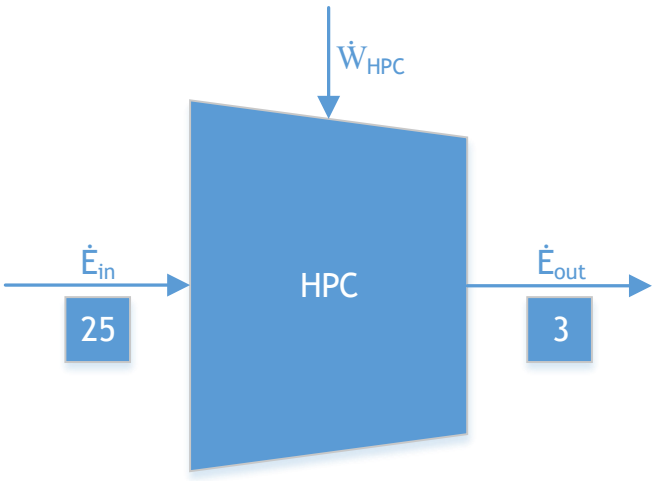

Figure 10: Exergy flows in the HPC.

$$\dot{m}_{25} = \dot{m}_3 \tag{116}$$

$$-\dot{w}_{HPC} + \dot{m}_{25}h_{25} - \dot{m}_3 h_3 = 0 \tag{117}$$

$$\dot{w}_{HPC} + \dot{E}_{25} - \dot{E}_3 - \dot{E}_{D,HPC} = 0 \tag{118}$$

$$\varepsilon_{HPC} = \frac{\dot{E}_3 - \dot{E}_{25}}{\dot{w}_{HPC}} \tag{119}$$

$$\dot{IP}_{HPC} = \dot{E}_{D,HPC}(1 - \varepsilon_{HPC}) \tag{120}$$

$$\chi_{HPC} = \frac{\dot{E}_{D,HPC}}{\sum \dot{E}_D} \tag{121}$$

$$\delta_{HPC} = \frac{\dot{E}_{D,HPC}}{\sum \dot{E}_F} \tag{122}$$

$$\xi_{HPC} = \frac{\dot{E}_{D,HPC}}{\sum \dot{E}_P} \tag{123}$$

➢ Combustion Chamber

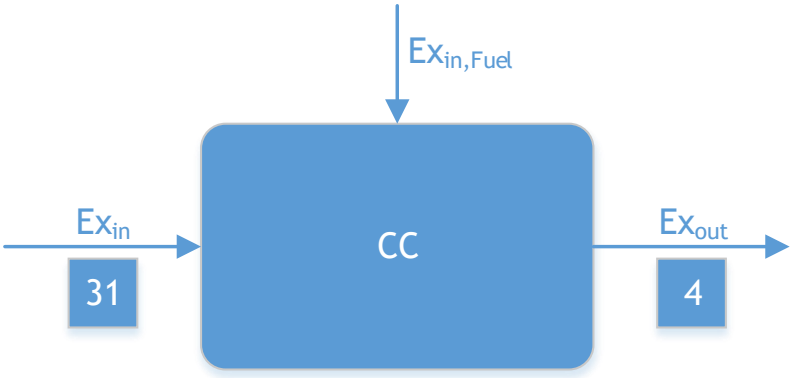

Figure 11: Exergy flows in CC.

$$\dot{m}_{31} + \dot{m}_{fuel} = \dot{m}_4 \tag{124}$$

$$\dot{m}_{31} h_{31} + \dot{m}_{fuel} LHV \eta_c - \dot{m}_4 h_4 = 0 \tag{125}$$

$$\dot{E}_{31} + \dot{E}_{fuel} - \dot{E}_4 - \dot{E}_{D,CC} = 0 \tag{126}$$

$$\varepsilon_{CC} = \frac{\dot{E}_4}{\dot{E}_{fuel} + \dot{E}_{31}} \tag{127}$$

$$I\dot{P}_{CC} = \dot{E}_{D,CC}(1 - \varepsilon_{CC}) \tag{128}$$

$$\chi_{CC} = \frac{\dot{E}_{D,CC}}{\sum \dot{E}_D} \tag{129}$$

$$\delta_{CC} = \frac{\dot{E}_{D,CC}}{\sum \dot{E}_F} \tag{130}$$

$$\xi_{CC} = \frac{\dot{E}_{D,CC}}{\sum \dot{E}_P} \tag{131}$$

➢ High Pressure Turbine

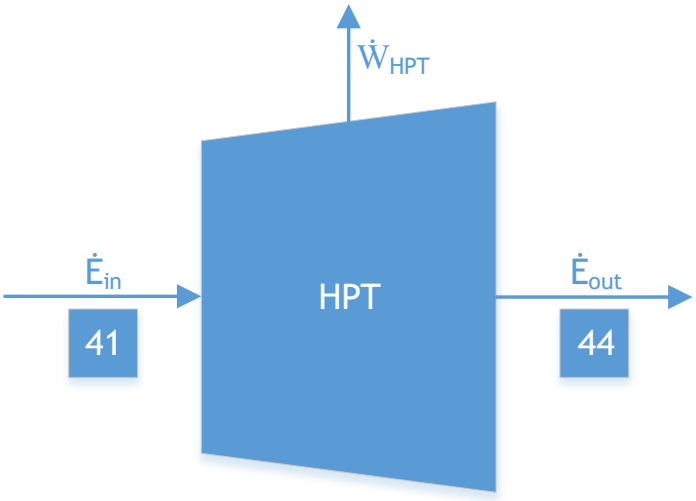

Figure 12: Exergy flows in HPT.

$$\dot{m}_{41} = \dot{m}_{44} \tag{132}$$

$$-\dot{w}_{HPT} + \dot{m}_{41}h_{41} - \dot{m}_{44}h_{44} = 0 \tag{133}$$

$$\dot{E}_{41} - \dot{w}_{HPT} - \dot{E}_{44} - \dot{E}_{D,HPT} = 0 \tag{134}$$

$$\varepsilon_{HPT} = \frac{\dot{w}_{HPT}}{\dot{E}_{41} - \dot{E}_{44}} \tag{135}$$

$$I\dot{P}_{HPT} = \dot{E}_{D,HPT}(1 - \varepsilon_{HPT}) \tag{136}$$

$$\chi_{HPT} = \frac{\dot{E}_{D,HPT}}{\sum \dot{E}_D} \tag{137}$$

$$\delta_{HPT} = \frac{\dot{E}_{D,HPT}}{\sum \dot{E}_F} \tag{138}$$

$$\xi_{HPT} = \frac{\dot{E}_{D,HPT}}{\sum \dot{E}_P} \tag{139}$$

- Low Pressure Turbine

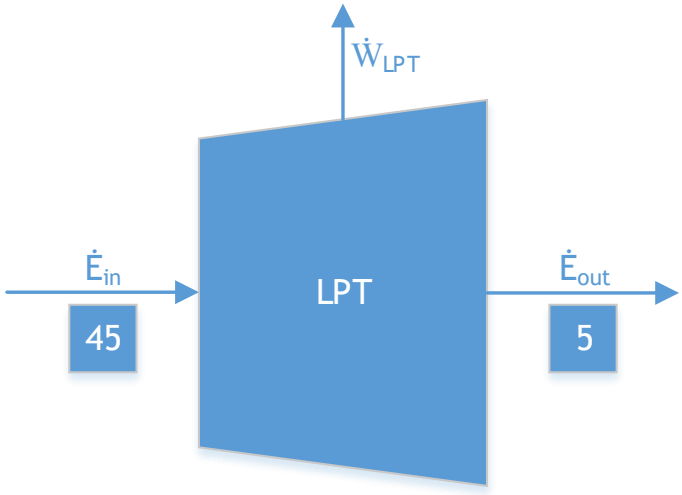

Figure 13: Exergy flows in LPT.

$$\dot{m}_{45} = \dot{m}_5 \tag{140}$$

$$-\dot{w}_{LPT} + \dot{m}_{45}h_{45} - \dot{m}_5 h_5 = 0 \tag{141}$$

$$\dot{E}_{45} - \dot{w}_{LPT} - \dot{E}_5 - \dot{E}_{D,LPT} = 0 \tag{142}$$

$$\varepsilon_{LPT} = \frac{\dot{w}_{LPT}}{\dot{E}_{45} - \dot{E}_5} \tag{143}$$

$$\dot{IP}_{LPT} = \dot{E}_{D,LPT}(1 - \varepsilon_{LPT}) \tag{144}$$

$$\chi_{LPT} = \frac{\dot{E}_{D,LPT}}{\sum \dot{E}_D} \tag{145}$$

$$\delta_{LPT} = \frac{\dot{E}_{D,LPT}}{\sum \dot{E}_F} \tag{146}$$

$$\xi_{LPT} = \frac{\dot{E}_{D,LPT}}{\sum \dot{E}_P} \tag{147}$$

6 Results and Discussion

The exergy analysis has been performed, by considering and applying the basic exergy formulas in Chapter 4 and governing equations in Chapter 5.

Figure 14 demonstrates the inlet and outlet exergy in each component of the engine. The components with more noticeable variations between the inlet and outlet exergy are the CC, HPT and LPT.

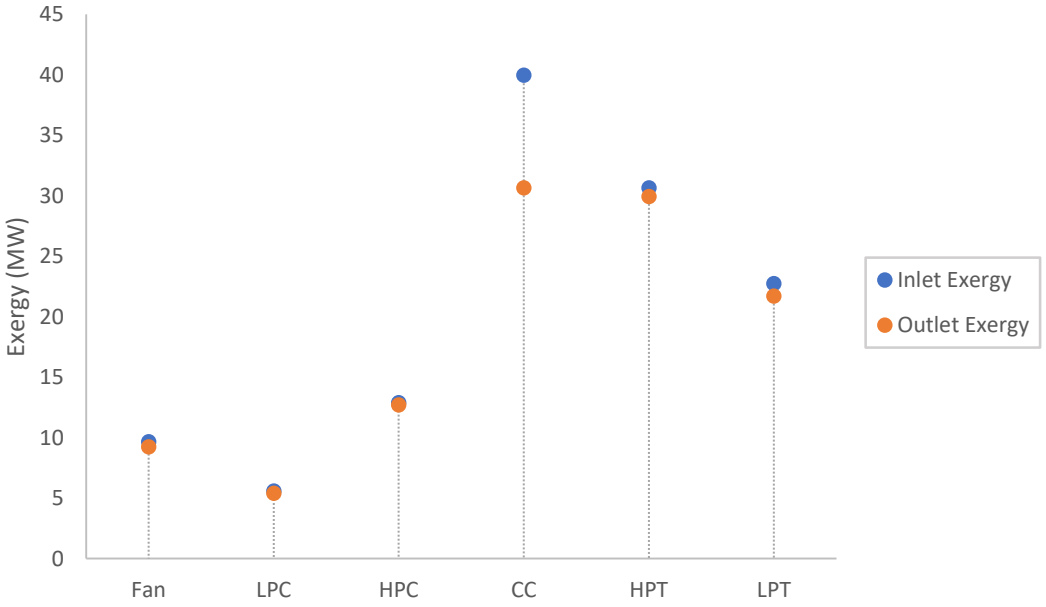

Figure 14: Exergy balance of the CFM56-5A1 engine components.

Figure 15 shows the inlet and outlet flows of the exergy components, i.e. the physical and chemical exergy, in each component of the engine. In the CC, it is clearly visible the contribution of the chemical exergy generated from the combustion process. In this component, the outlet physical exergy is very superior in respect with the inlet physical exergy due to the temperature rise triggered by the combustion process.

Figure 16 demonstrates the distribution of the exergy components in the engine components. Physical exergy is responsible for the majority, 88%, while the chemical exergy only accounts with 12%. The main source of chemical exergy in the engine comes from the combustion process in the CC.

Figure 17 demonstrates the distribution of the exergy components in the CC. Physical exergy accounts with 61% and chemical exergy with 39%. Excluding the exergy in the CC, the majority exergy available in the rest of the engine is in the form of physical exergy, with 99% and the

chemical exergy with only 1% (Figure 18). Chemical exergy is minimal in the rest of the engine since there are no others chemical reactions.

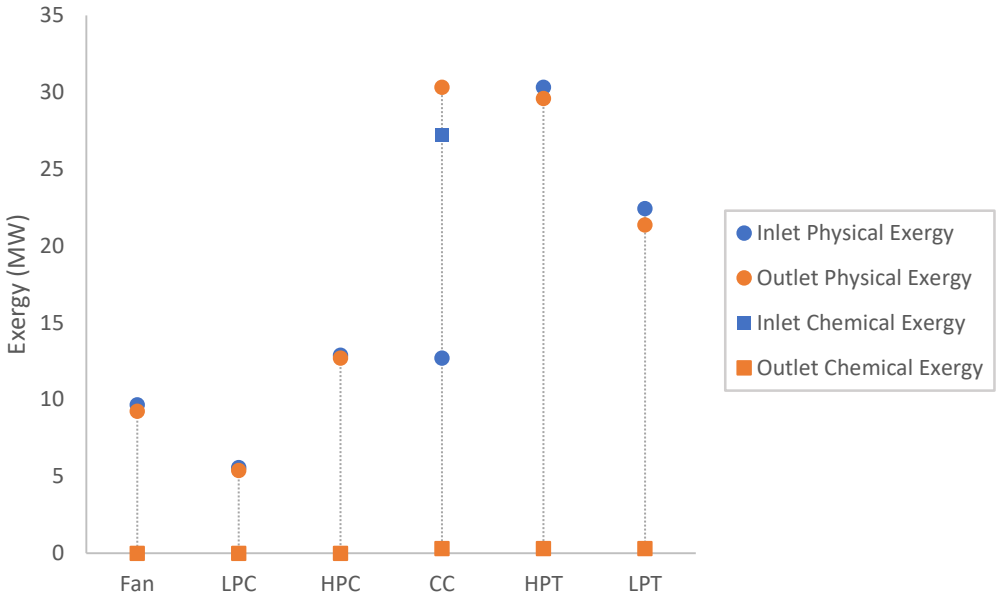

Figure 15: Physical and chemical exergy balances in the CFM56-5A1 engine components.

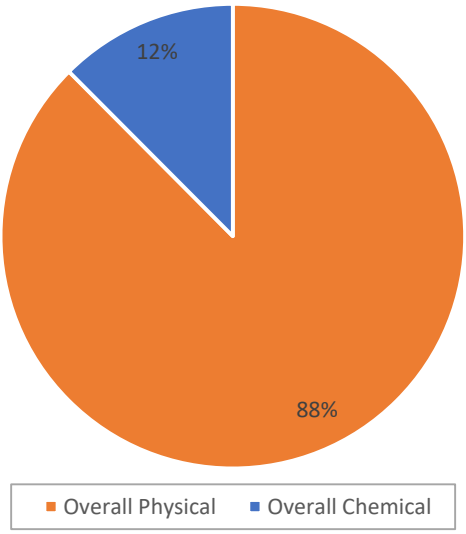

Figure 16: Physical and chemical exergy distribution in the CFM56-5A1 engine components.

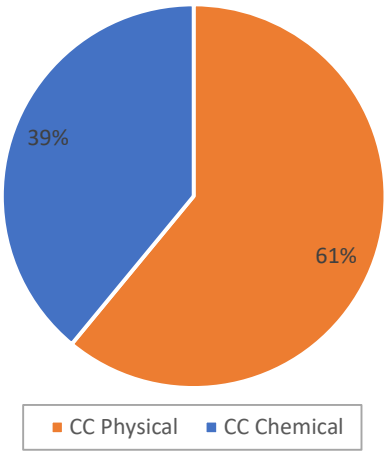

Figure 17: Physical and chemical exergy in the CC.

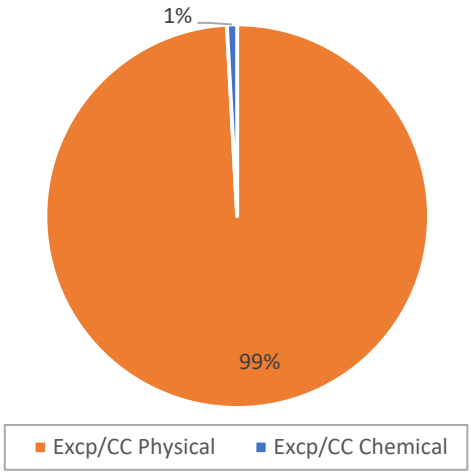

Figure 18: Physical and chemical exergy in CFM56-5A1 components, excluding the CC.

Figure 19 shows the exergy efficiency in the components of the engine. The most inefficient component was found to be the CC. The other components reveal a relative good exergy efficiency (>90%). The exergy efficiency for the Fan, LPC, HPC, CC, HPT, LPT are found to be 92.13%, 95.91%, 97.52%, 76.71%, 90.74%, 90.32%, respectively.

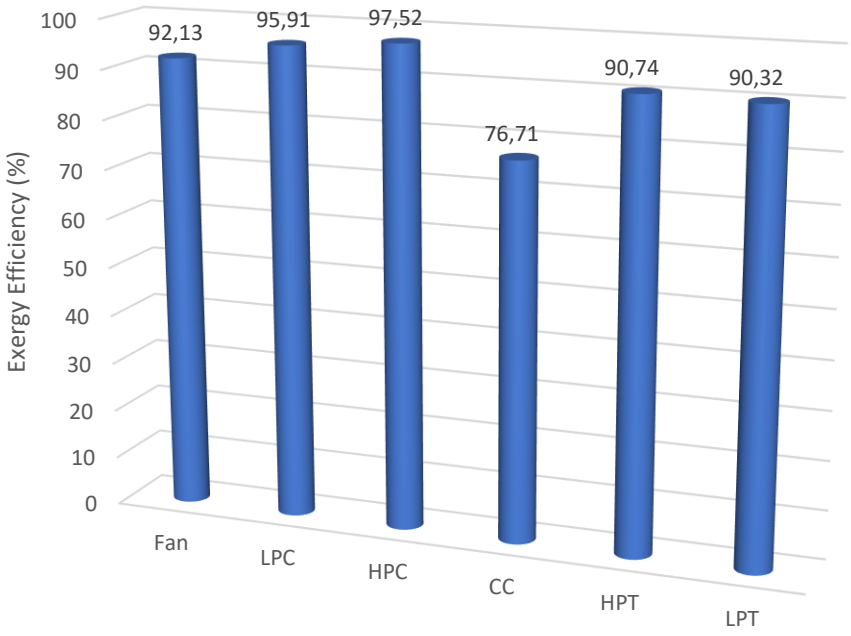

Figure 19: Exergy efficiency of the CFM56-5A1 engine components.

Figure 20 presents the exergy destruction in the components of the engine. As expected, by considering its exergy efficiency, the CC has the most exergy destruction. The exergy destruction for the Fan, LPC, HPC, CC, HPT, LPT are found to be 0.43 MW, 0.17 MW, 0.19 MW, 9.31 MW, 0.73 MW, 1.05 MW, respectively.

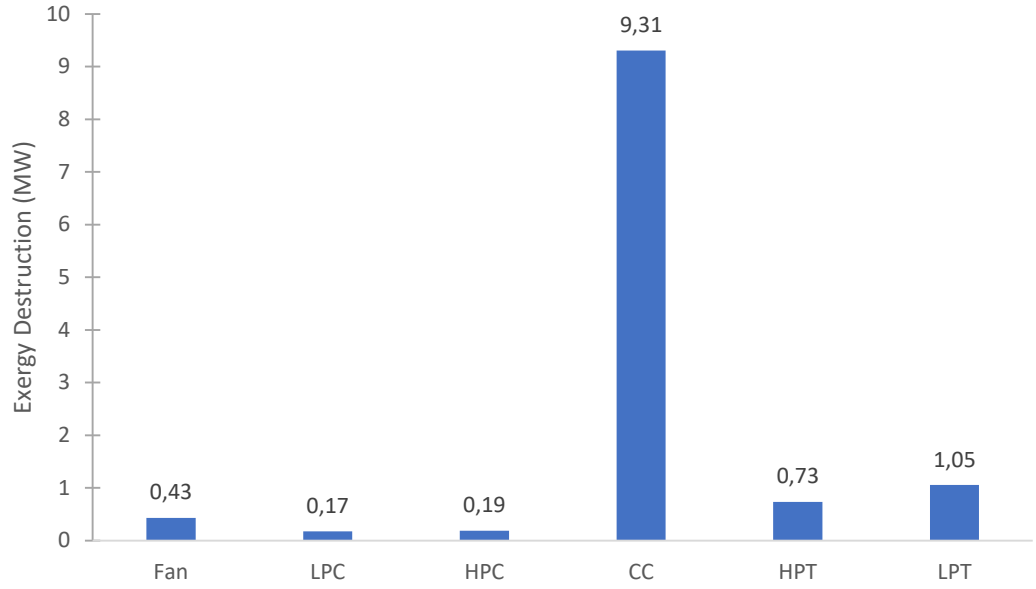

Figure 20: Exergy destruction of the CFM56-5A1 engine components.

Figure 21 demonstrates the improvement potential in each component of the engine. This is another important figure of merit, since it shows the magnitude of the exergy that can be improved. The most promising component to be improved is the CC. The improvement potential for the Fan, LPC, HPC, CC, HPT, LPT are found to be 0.03 MW, 0.01, MW, 0.005 MW, 2.17 MW, 0.07 MW, 0.10 MW, respectively.

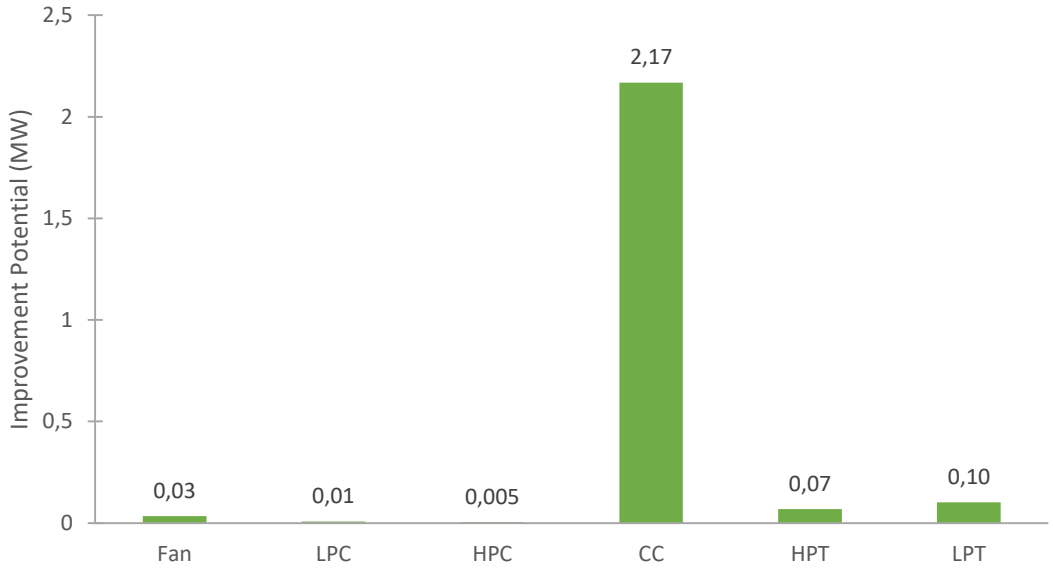

Figure 21: Improvement potential of the CFM56-5A1 engine components.

Figure 22 shows the relative exergy destruction in each component of the engine. Once again, the CC is the component which presents the most exergy destruction within the engine in

comparison with the other components. The relative destruction rate for the Fan, LPC, HPC, CC, HPT, LPT are found to be 3.63%, 1.47%, 1.56%, 78.30%, 6.17%, 8.87%, respectively.

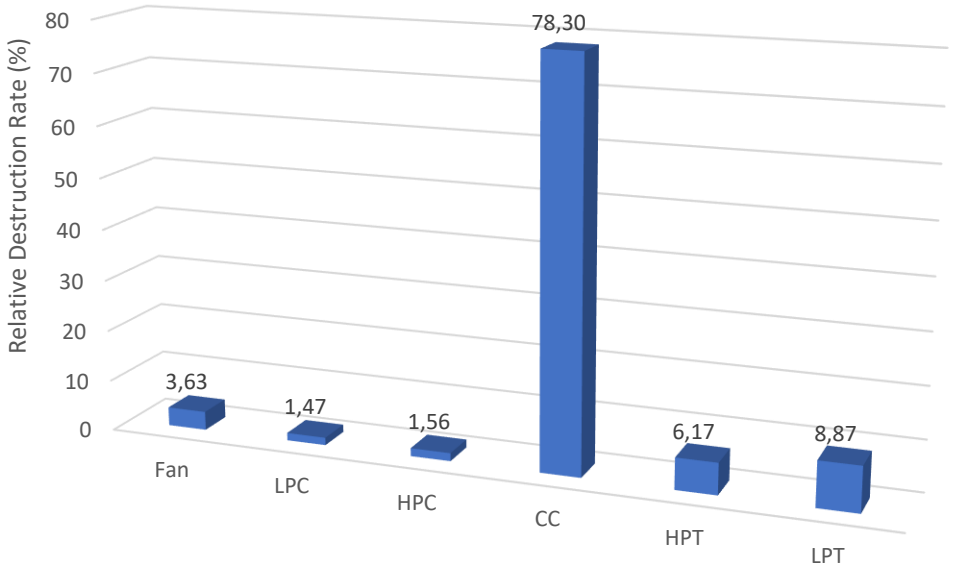

Figure 22: Relative exergy destruction of the CFM56-5A1 engine components.

Figures 23 and 24 presents the fuel depletion rate and productivity lack rate within the engine, respectively. The CC is the component with most fuel depletion and lack of productivity. The fuel depletion rate for the fan, LPC, HPC, CC, HPT, LPT are found to be 0.30%, 0.12%, 0.13%, 6.41%, 0.50%, 0.73%, respectively. The productivity lack ratio for the fan, LPC, HPC, CC, HPT, LPT are found to be 0.68%, 0.27%, 0.29%, 14.85%, 1.28%, 1.66%, respectively.

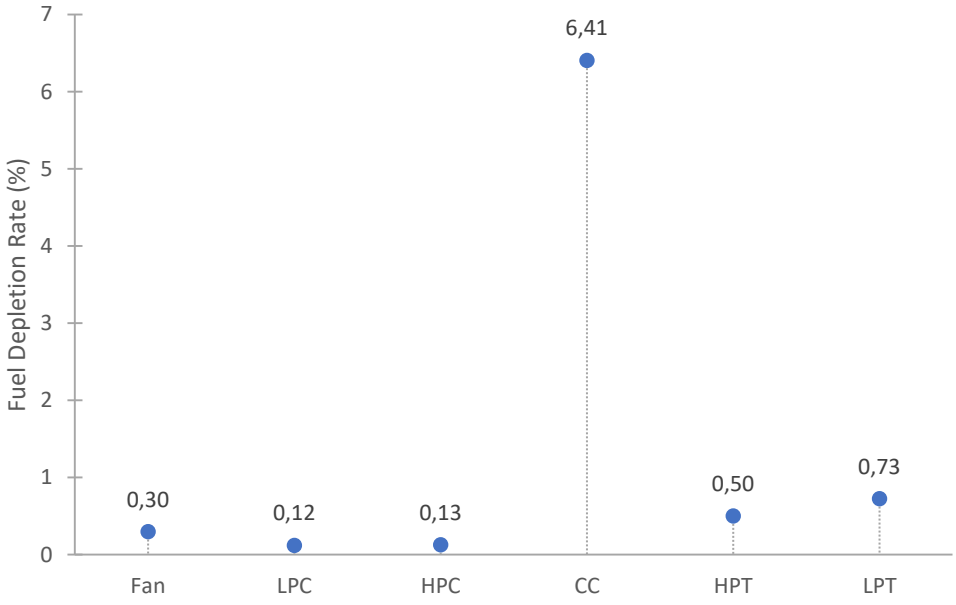

Figure 23: Fuel depletion rate of the CFM56-5A1 engine components.

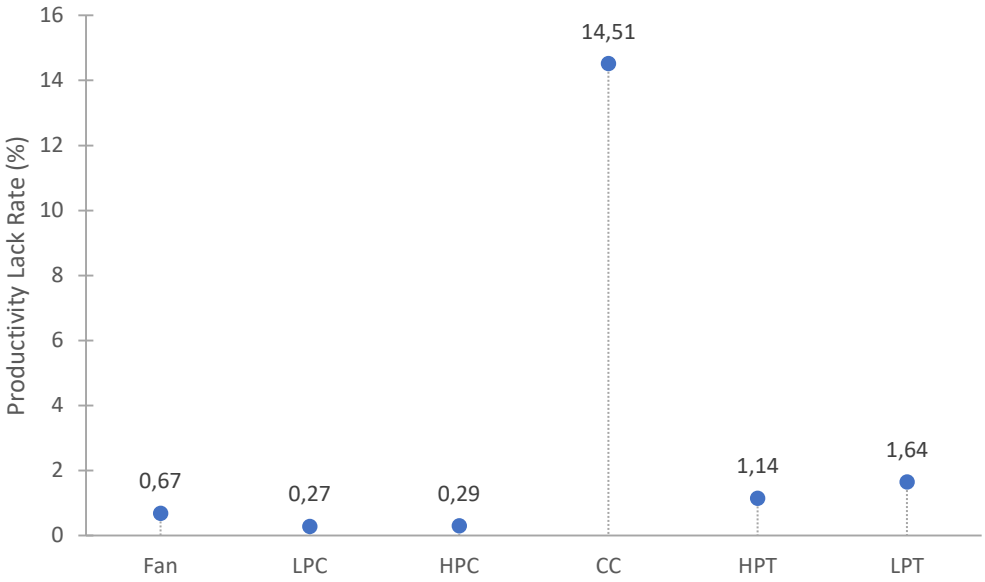

Figure 24: Productivity lack ratio of the CFM56-5A1 engine components.

The overall exergetic performance of the engine is displayed in Figure 25.

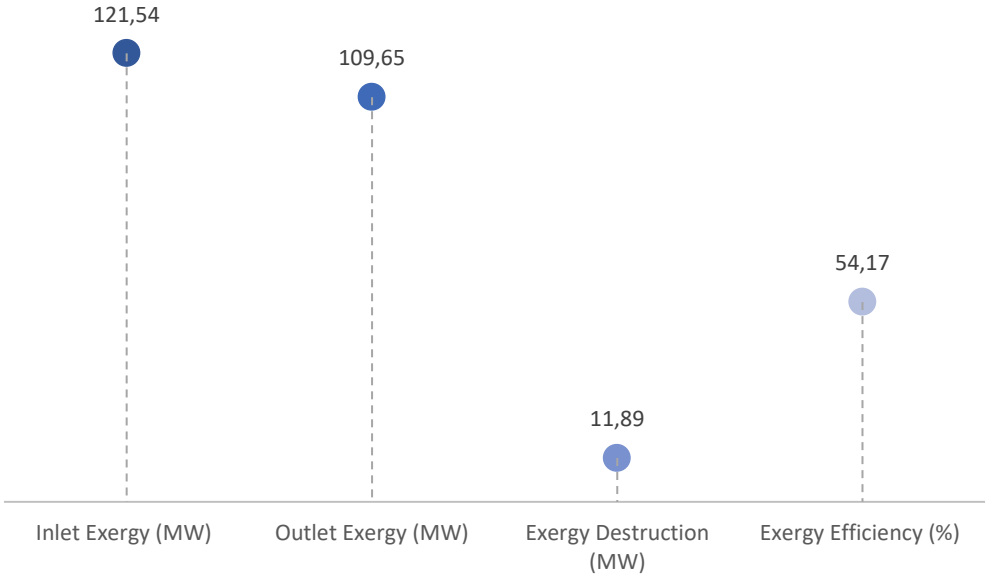

Figure 25: Overall exergetic performance of the CFM56-5A1 engine.

The summarized exergy parameters referred in this analysis are listed in Table 11.

Table 11: Exergy parameters of the CFM56-5A1 engine components.

Component	Exergy In (MW)	Exergy Out (MW)	Exergy Destruction (MW)	$\varepsilon(\%)$	$\dot{IP}$ (MW)	$\chi(\%)$	$\delta(\%)$	$\xi(\%)$
Fan	9.68	9.25	0.43	92.13	0.03	3.56	0.30	0.68
LPC	5.58	5.41	0.17	95.91	0.01	1.44	0.12	0.27
HPC	12.91	12.72	0.19	97.52	0.005	1.53	0.13	0.29
CC	39.96	30.65	9.31	76.71	2.17	78.30	6.41	14.51
HPT	30.35	29.92	0.73	90.74	0.07	6.17	0.50	1.14
LPT	22.54	21.70	1.05	90.32	0.10	8.87	0.77	1.64

7 Conclusion

The aim of this thesis was to perform an exergy analysis of a turbofan engine with the objective of providing a realistic and meaningfully understanding of the inefficiencies and destructions of exergy within the engine.

From the exergy analysis of the CFM56-5A1 engine, several conclusions could be drawn:

- Employing exergy analysis provided a realistic first and second law of thermodynamics evaluation of the engine.
- The main irreversible component of the engine is found to be the combustion chamber with 9.31 MW of exergy destruction.
- The chemical exergy didn't produce a significant impact in the analysis, with the exception of the CC. The main source of chemical exergy in the engine comes from the combustion process in the combustion chamber. In the other components, the chemical exergy is significantly low since there are no others chemical reactions. The exergy analysis is mostly based on physical exergy.
- The CFM56-5A1 proved to be a well engineered and designed engine, in respect with the cruise operating conditions. The exergetic efficiencies of the components were superior to 90%, except for the combustion chamber with 76.71% of exergetic efficiency.
- The most promising component to be improved is found to be the combustion chamber with an improvement potential of 2.17 MW. The other components have a relatively low improvement potential.
- Naturally, by reducing exergy destruction of the engine components and increasing the exergetic efficiencies will result in reduced emissions, less environmental impact and enhanced sustainability.

7.1 Future Works

This thesis made a big step in exergy analysis of aircraft engines. There are improvement potentials in the engine, particularly, in the combustion chamber.

In this thesis, an exergoeconomic analysis has not been done. By using the exergoeconomic analysis method for a future work, it could decide whether using more advanced and more expensive turbo machineries cost is offset by the decreasing exergy destruction.

Another study to be considered, is an exergetic optimization of the CFM56-5A1 by changing the design dimensions and variables within the engine. However, it would be necessary to perform an exergoeconomic analysis to make sure the optimization would bring cost benefits to the manufacturer.

References

[1] ICAO (2017),” Forecasts of Scheduled Passenger and Freight Traffic”, Accessed 5 July 2017

https://www.icao.int/sustainability/pages/eap_fp_forecastmed.aspx

[2] IPPC (2007), “Climate Change 2007: Synthesis Report”, Accessed 5 July 2017

http://www.ipcc.ch/pdf/assessment-report/ar4/syr/ar4_syr.pdf

[3] Dincer, Ibrahim, and Rosen, Marc, “Exergy: Energy, Environment and Sustainable Development”, Elsevier, Second Edition, 2013, pp. 6-78, ISBN: 978-0-08-097089-9

[4] Dincer, Ibrahim, et al, “Progress in Exergy, Energy, and the Environment”, Springer, First Edition, 2014, pp. 293-305, ISBN 978-3-319-04680-8

[5] Tatiana, M., and Tsatsaronis, G, “Advanced Exergy Analysis for Chemically Reacting Systems: Application to a Simple Open Gas-Turbine System”, International Journal of Thermodynamics, Vol. 12, 2009, pp. 105-111, ISSN 1301-9724

[6] Habib, M. “First and Second-Law Analysis of Steam Turbine Cogeneration Systems”, Journal of Engineering for Gas Turbine and Power, Vol. 116, 1994, pp. 15-19, ISSN 1290-6786

[7] Altayi, Khalid, “Energy, Exergy and Exergoeconomic Analyses of Gas-Turbine Based System”, Master´s Thesis, University of Ontario Institute of Technology, Canada, 2011

[8] Sohret, Yasin, et al, “Exergy analysis of a turbofan engine for an unmanned aerial vehicle during a surveillance mission”, Elsevier, 2015, pp. 716-729, ISSN 0360-5442

[9] Etele, Jason, and Rosen, M., "Sensitivity of exergy efficiencies of aerospace engines to reference environment selection". Exergy International Journal,Vol. 1, 2001, pp. 91-99, ISSN 1164-0235

[10] Safran, “Commercial Aircraft Engines: CFM56-5A”, Accessed 13 July 2017

https://www.safran-aircraft-engines.com/file/download/fiche_cfm56 5a_ang2011.pdf

[11] EASA, “EASA Type Certificate: CFM56-5A1”, Accessed 15 July 2017

https://www.easa.europa.eu/system/files/dfu/EASA-TCDS-E.067_CFM___International_S.A._--_CFM56--5_series_engines-01-18052009.pdf

[12] Safran, “Aircraft and engine nacelles”, Accessed 15 July 2017

https://www.safran-group.com/aviation/aircraft-engines-and-nacelles/aircraft-engines

[13] Nasa, “Brayton Cycle”, Accessed 16 July 2017

https://www.grc.nasa.gov/www/k-12/airplane/Images/braytonts.gif

[14] Jet Engine, “Civil Aircraft Engine Database”, Accessed 18 July 2017

http://www.jet-engine.net

[15] Lufthansa, “Training Manual A319/A320/A321”, Accessed 22 July 2017

https://www.metabunk.org/attachments/docslide-us_a-320-engine-pdf.16733/

[16] Gasturb, “Gasturb Engine Database”, Accessed 23 July 2017

http://www.gasturb.de/Gtb13Manual/GasTurb13.pdf

[17] Walsh, P., and Fletcher, P., “Gas Turbine Performance”, Second Edition, 2004, Blackwell Science Ltd, ISBN: 978-0632064342

[18] Dincer, Ibrahim, et al, “Optimization of Energy Systems”, Wiley, First Edition, 2017, pp. 5-30, ISBN 9781118894439

[19] ÇolPan, C., “Exergy Analysis of Combined Cycle Cogeneration Systems”, Master`s Thesis, Middle East Technical University, Turkey, 2005

[20] Kotas, T., “The exergy Method of Thermal Plant Analysis”, Elsevier, First Edition, 1985, pp. 127-129, ISBN 9781483100364

[21] Isidoro Martinez (2017), “Chemical Exergy”, Accessed 13 August 2007

http://webserver.dmt.upm.es/~isidoro/dat1/Chemical%20exergy.pdf

[22] Balli, Ozgur, “Energetic and exergetic analyses of T56 turboprop engine”, Elsevier, 2013, pp. 106-120, ISSN 0196-8904

[23] Larry Caretto (2010), “Introduction to Combustion Analysis”, Accessed 15 August 2017

http://www.csun.edu/~lcaretto/me483/combustion.pdf

[24] Flagan, Richard (2008), “Removal of Gaseous Pollutants from Effluent Streams”, Accessed 15 August 2017

https://authors.library.caltech.edu/25069/10/AirPollution88-Ch8.pdf